

PREPARED FOR SUBMISSION TO JHEP

Surface operators, dual quivers and contours

**S. K. Ashok,^a S. Ballav,^a M. Billò,^{b,c} E. Dell'Aquila,^b M. Frau,^{b,c} V. Gupta,^a
R. R. John,^{b,c} and A. Lerda^{d,c}**

^a*Institute of Mathematical Sciences
Homi Bhabha National Institute (HBNI)
IV Cross Road, C. I. T. Campus,
Taramani, Chennai, 600113 Tamil Nadu, India*

^b*Università di Torino, Dipartimento di Fisica*

^c*Arnold-Regge Center and I. N. F. N. - sezione di Torino,
Via P. Giuria 1, I-10125 Torino, Italy*

^d*Università del Piemonte Orientale, Dipartimento di Scienze e Innovazione Tecnologica
Viale T. Michel 11, I-15121 Alessandria, Italy*

E-mail: sashok@imsc.res.in, sballav@imsc.res.in, billò@to.infn.it,
edellaquila@gmail.com, frau@to.infn.it, varungupta@imsc.res.in,
renjan.rajan@to.infn.it, lerda@to.infn.it

ABSTRACT: We study half-BPS surface operators in four dimensional $\mathcal{N} = 2$ $SU(N)$ gauge theories. We calculate the ramified instanton partition function using equivariant localization and extract the low-energy effective action on the four dimensional Coulomb branch. We also study surface operators as coupled 2d/4d quiver gauge theories with an $SU(N)$ flavour symmetry. In this description, the same surface operator can be described by different quivers that are related to each other by two dimensional Seiberg duality. We argue that these dual quivers correspond, on the localization side, to distinct integration contours that can be determined by the relative magnitudes of the Fayet-Iliopoulos parameters of the two dimensional gauge nodes and by the signs of their β -functions. We verify the proposal by mapping the solutions of the twisted chiral ring equations of the 2d/4d quivers onto individual residues of the localization integrand.

KEYWORDS: Supersymmetric gauge theories, ramified instantons, surface operators, duality

Contents

1	Introduction	1
2	Review of earlier work	3
2.1	Surface operators as monodromy defects	3
2.2	Surface operators as coupled 2d/4d quivers	5
2.3	A contour from the twisted chiral ring	6
3	2d Seiberg duality	9
4	Relating quivers and contours	11
4.1	Contour prescriptions for dual quivers	16
4.2	The Jeffrey-Kirwan prescription for dual quivers	19
4.3	Proposal for generic linear quivers	21
5	New quivers and the corresponding contours	22
6	Summary of results	24
A	Localization results at one-instanton level	26
B	Chiral ring equations and superpotentials at the one-instanton level	28
C	Some two-instanton results	36

1 Introduction

Surface operators in 4d gauge theories are natural two dimensional generalizations of Wilson and 't Hooft loops which can provide valuable information about the phase structure of the gauge theories [1]. In this paper we study the low-energy effective action of surface operators in pure $\mathcal{N} = 2$ gauge theories in 4d from two distinct points of view, namely as monodromy defects [2, 3] and as coupled 2d/4d quiver gauge theories [4, 5]. In the first approach, one specifies how the 4d gauge fields are affected by the presence of the surface operator by imposing suitable boundary conditions in the path-integral. In this framework the non-perturbative effects are described in terms of ramified instantons [2] whose partition function can be computed using equivariant localization methods [5–10]. From the ramified instanton partition function one can extract two holomorphic functions [11, 12]: one is the prepotential \mathcal{F} that governs the low-energy effective action of the 4d $\mathcal{N} = 2$ gauge theory on the Coulomb branch; the other is the twisted chiral superpotential \mathcal{W} that describes the 2d dynamics on the defect.

In the second description of the surface operators, one considers coupled 2d/4d theories that are $(2, 2)$ supersymmetric sigma models with an ultraviolet description as a gauged linear sigma model (GLSM). The low-energy dynamics of such a GLSM is completely determined by a twisted chiral superpotential $\mathcal{W}(\sigma)$ that depends on the twisted chiral superfields σ containing the 2d vector fields [13]. By giving a vacuum expectation value (v.e.v.) to the adjoint scalar of the 4d $\mathcal{N} = 2$ gauge theory, one introduces twisted masses in the 2d quiver theory [14, 15]. At a generic point on the 4d Coulomb branch, the 2d theory is therefore massive in the infrared and the 2d/4d coupling mechanism is determined via the resolvent of the 4d gauge theory [5]. The resulting massive vacua of the GLSM are solutions to the twisted chiral ring equations, which are obtained by extremizing $\mathcal{W}(\sigma)$ with respect to the twisted chiral superfields.

The main goal of this work is to clarify the precise relationship between the above two descriptions of the surface operators and provide a dictionary to map calculable quantities on one side to the other. In our previous works [9, 10] the first steps in this direction were already taken by showing that there is a precise correspondence between the massive vacua of the 2d/4d gauge theory and the monodromy defects in the $\mathcal{N} = 2$ gauge theory. In fact, the effective twisted chiral superpotential of the 2d/4d quiver gauge theory evaluated in a given massive vacuum exactly coincides with the one computed from the 4d ramified instanton partition function [9, 10]. This equality was shown in a specific class of models that are described by oriented quiver diagrams. Recently, this result has been proven in full generality in [16, 17].

An important feature of the $(2, 2)$ quiver theories that was not fully discussed in our previous papers is Seiberg duality [18, 19]. This is an infrared equivalence between two gauge theories that have different ultraviolet realizations. In this work we fill this gap and consider all possible quivers obtained from the oriented ones by applying 2d Seiberg duality. While all such quivers have different gauge groups and matter content, once the 4d Coulomb v.e.v.'s are turned on, it is possible to find a one-to-one map between their massive vacua. Therefore it becomes clear that they must describe the same surface operator from the point of view of the 4d gauge theory; indeed, the different twisted chiral superpotentials, evaluated in the respective vacua, all give the same result. This equality of superpotentials gives a strong hint that the choice of a Seiberg duality frame might have an interpretation as distinct contours of integration on the localization side: the equality of the superpotentials would then be a simple consequence of multi-dimensional residue theorems.

In this work we show that this expectation is correct and provide a detailed map between a given quiver realization of the surface operator and a particular choice of contour in the localization integrals. This contour prescription can be conveniently encoded in a Jeffrey-Kirwan (JK) reference vector [20]. The JK vector, in turn, is uniquely determined by the relative magnitudes of Fayet-Iliopoulos (FI) parameters or, equivalently, by the hierarchy of strong coupling scales in the quantum 2d/4d quiver gauge theory. While the twisted superpotentials are equal irrespective of the choice of contour, the map relates the individual residues on the localization side to the individual terms in the solutions to the twisted chiral ring equations, thereby allowing us to identify in an unambiguous way which

quiver arises from a given contour prescription and vice-versa.

This paper is organized as follows. In Section 2 we review and extend our earlier work [8–10], and in particular we show how to map the oriented quiver to a particular contour by studying the solution of the chiral ring equations and the precise correspondence to the residues of the localization integrand. In Section 3 we discuss the basics of 2d Seiberg duality and how it acts on the quiver theories we consider. In Sections 4 and 5 we apply the duality moves to the 2d/4d quivers of interest and show in detail how it is possible to map each quiver to a particular integration contour on the localization side without explicitly solving the chiral ring equations. We also discuss how this integration contour can be specified in terms of a JK reference vector. Finally, we summarize our main results in Section 6 and collect the more technical material in the appendices.

2 Review of earlier work

To set the stage for the discussion in the next sections and also to introduce our notation, we briefly review the results obtained in our earlier work [10] where we studied surface operators both as monodromy defects in 4d and as coupled 2d/4d gauge theories.

2.1 Surface operators as monodromy defects

As a monodromy defect, a surface operator in a 4d $SU(N)$ theory is specified by a partition of N , denoted by $\vec{n} = [n_1, n_2, \dots, n_M]$, which corresponds to the breaking of the gauge group to a Levi subgroup

$$\mathbb{L} = S[U(n_1) \times U(n_2) \times \dots \times U(n_M)] \quad (2.1)$$

at the location of the defect [2, 3]. This also gives a natural partitioning of the classical Coulomb v.e.v.'s of the adjoint scalar Φ of the $\mathcal{N} = 2$ $SU(N)$ theory as follows:

$$\langle \Phi \rangle = \{a_1, \dots, a_{r_1} | \dots | a_{r_{I-1}+1}, \dots, a_{r_I} | \dots | a_{r_{M-1}+1}, \dots, a_N\} . \quad (2.2)$$

Here we have defined the integers r_I according to

$$r_I = \sum_{J=1}^I n_J , \quad (2.3)$$

so that the I^{th} partition in (2.2) is of length n_I . Introducing the following set of numbers with cardinality n_I :

$$\mathcal{N}_I \equiv \{r_{I-1} + 1, r_{I-1} + 2, \dots, r_I\} , \quad (2.4)$$

we define the $n_I \times n_I$ block-diagonal matrices \mathcal{A}_I according to

$$\mathcal{A}_I \equiv \text{diag} (a_{s \in \mathcal{N}_I}) = \begin{pmatrix} a_{r_{I-1}+1} & 0 & 0 & \dots \\ 0 & \ddots & 0 & \dots \\ \vdots & \vdots & \ddots & \\ 0 & 0 & \dots & a_{r_I} \end{pmatrix} . \quad (2.5)$$

With these conventions, the splitting in (2.2) can be written as

$$\langle \Phi \rangle = \mathcal{A}_1 \oplus \mathcal{A}_2 \oplus \dots \oplus \mathcal{A}_M . \quad (2.6)$$

The instanton partition function in the presence of such a surface operator, also known as the ramified instanton partition function, takes the following form [6, 10]:

$$Z_{\text{inst}}[\vec{n}] = \sum_{\{d_I\}} Z_{\{d_I\}}[\vec{n}] \quad \text{with} \quad Z_{\{d_I\}}[\vec{n}] = \prod_{I=1}^M \left[\frac{(-q_I)^{d_I}}{d_I!} \int \prod_{\sigma=1}^{d_I} \frac{d\chi_{I,\sigma}}{2\pi i} \right] z_{\{d_I\}} \quad (2.7)$$

where

$$\begin{aligned} z_{\{d_I\}} = & \prod_{I=1}^M \prod_{\sigma,\tau=1}^{d_I} \frac{(\chi_{I,\sigma} - \chi_{I,\tau} + \delta_{\sigma,\tau})}{(\chi_{I,\sigma} - \chi_{I,\tau} + \epsilon_1)} \times \prod_{I=1}^M \prod_{\sigma=1}^{d_I} \prod_{\rho=1}^{d_{I+1}} \frac{(\chi_{I,\sigma} - \chi_{I+1,\rho} + \epsilon_1 + \hat{\epsilon}_2)}{(\chi_{I,\sigma} - \chi_{I+1,\rho} + \hat{\epsilon}_2)} \\ & \times \prod_{I=1}^M \prod_{\sigma=1}^{d_I} \frac{1}{\prod_{s \in \mathcal{N}_I} (a_s - \chi_{I,\sigma} + \frac{1}{2}(\epsilon_1 + \hat{\epsilon}_2))} \frac{1}{\prod_{t \in \mathcal{N}_{I+1}} (\chi_{I,\sigma} - a_t + \frac{1}{2}(\epsilon_1 + \hat{\epsilon}_2))} . \end{aligned} \quad (2.8)$$

Here, the M positive integers d_I count the numbers of ramified instantons in the various sectors, the variables q_I are the ramified instanton weights, and the parameters ϵ_1 and $\hat{\epsilon}_2 = \epsilon_2/M$ specify the Ω -background [21, 22] which is introduced to localize the integrals over the instanton moduli space¹.

There is one more ingredient that is needed to calculate the partition function (2.7), namely the contour of integration for the χ_I variables. A convenient way to specify it and to select which poles of the integrand contribute and which do not, is to treat the Coulomb v.e.v.'s a as real variables and assign an imaginary part to the Ω -deformation parameters according to

$$0 < \text{Im}(\hat{\epsilon}_2) \ll \text{Im}(\epsilon_1) \ll 1 . \quad (2.9)$$

Then, the contour is specified by integrating $\chi_{I,\sigma}$ in the upper or lower half-plane and by choosing a definite order in the successive integrations. Equivalently, as we will see in the following sections, the contour of integration can be selected by specifying a Jeffrey-Kirwan reference vector [20].

In the limit $\epsilon_1, \hat{\epsilon}_2 \rightarrow 0$, the low-energy effective action of the gauge theory with the 2d defect is specified by two holomorphic functions: the prepotential \mathcal{F} and the twisted chiral superpotential \mathcal{W} . Each of these functions can be written as a sum of the classical, the one-loop, and the instanton contributions. The latter can be extracted from the ramified instanton partition function as follows [11, 12]:

$$\log(1 + Z_{\text{inst}}) = -\frac{\mathcal{F}_{\text{inst}}}{\epsilon_1 \hat{\epsilon}_2} + \frac{\mathcal{W}_{\text{inst}}}{\epsilon_1} + \dots \quad (2.10)$$

where the ellipses refer to regular terms. In Appendix A we list the one-instanton contribution to $\mathcal{W}_{\text{inst}}$ calculated for various choices of contours in the case $M = 4$. As we will show in the following, the different contour prescriptions can be given a physical meaning by associating them to specific 2d/4d quiver gauge theories.

¹The rescaling by a factor of M in ϵ_2 is due to a \mathbb{Z}_M -orbifold projection that has to be performed in the ramified instanton case [6]. Furthermore, in (2.8) the sub-index I is always understood modulo M .

2.2 Surface operators as coupled 2d/4d quivers

The prepotential \mathcal{F} governs the 4d gauge theory dynamics at a generic point on the Coulomb branch. The twisted chiral superpotential \mathcal{W} , instead, is best understood as the low-energy effective description of a 2d non-linear sigma model. For a surface operator with a Levi subgroup \mathbb{L} in a 4d theory with a gauge group G , the relevant sigma model is defined on the target space G/\mathbb{L} [2, 3]. Such a space is, in general, a flag variety which can be realized as the low-energy limit of a GLSM [13, 15], whose gauge and matter content can be summarized in the quiver diagram of Fig. 1.

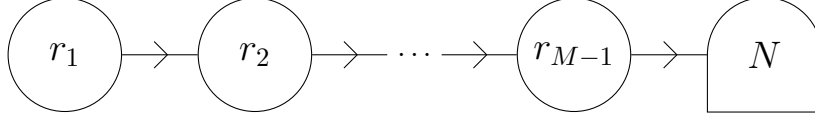


Figure 1. The quiver which describes the generic surface operator in pure $SU(N)$ gauge theory.

Each circular node represents a 2d gauge group $U(r_I)$ where the ranks r_I are as in (2.3), whereas the last node on the right hand side represents the 4d gauge group $SU(N)$ which acts as a flavour symmetry group for the $(M-1)^{\text{th}}$ 2d node. The arrows correspond to matter multiplets which are rendered massive by non-zero v.e.v's of the twisted scalars $\sigma^{(I)}$ of the I^{th} node and of the 4d adjoint scalar Φ . The orientation of the arrows specifies whether the matter is in the fundamental (out-going) or in the anti-fundamental (in-going) representation.

The effective action for the twisted chiral multiplets is obtained by integrating out the massive matter multiplets and, thanks to supersymmetry, can be encoded in the effective twisted chiral superpotential. For the quiver of Fig. 1, this is given by:

$$\mathcal{W} = 2\pi i \sum_{I=1}^{M-1} \sum_{s=1}^{r_I} \tau_I \sigma_s^{(I)} - \sum_{I=1}^{M-2} \sum_{s=1}^{r_I} \sum_{t=1}^{r_{I+1}} \varpi(\sigma_s^{(I)} - \sigma_t^{(I+1)}) - \sum_{s=1}^{r_{M-1}} \left\langle \text{Tr } \varpi(\sigma_s^{(M-1)} - \Phi) \right\rangle \quad (2.11)$$

where

$$\varpi(x) = x \left(\log \frac{x}{\mu} - 1 \right), \quad (2.12)$$

μ is the UV cut-off scale, and τ_I is the complexified FI parameter of the I^{th} node at the scale μ , namely

$$\tau_I = \frac{\theta_I}{2\pi} + i \zeta_I \quad (2.13)$$

with θ_I and ζ_I being, respectively, the θ -parameter and the real FI parameter of the I^{th} gauge node. Finally, the angular brackets in the last term of (2.11) correspond to a chiral correlator in the 4d $SU(N)$ theory. This correlator implies that the coupling between the 2d and 4d theory is via the resolvent of the $SU(N)$ gauge theory [5], which in turn depends on the 4d dynamically generated scale Λ_{4d} .

The running of the FI parameters leads to introducing 2d strong coupling scales Λ_I at each node by the relation

$$\Lambda_I^{b_I} = e^{2\pi i \tau_I} \mu^{b_I} \quad (2.14)$$

where b_I is the corresponding β -function coefficient, which in this case is

$$b_I = n_I + n_{I+1} . \quad (2.15)$$

In any linear quiver like the one represented in Fig. 1, we make the following choice for the hierarchy of scales:

$$|\Lambda_1| \gg |\Lambda_2| \gg \cdots \gg |\Lambda_{M-1}| \gg |\Lambda_{4d}| . \quad (2.16)$$

This ensures that we can decouple the nodes one by one, beginning with the 4d node and working a step at a time leftwards without breaking the quiver into disjoint parts. This choice will prove to be very convenient in the following sections.

Once the 4d Coulomb v.e.v.'s are given, the 2d Coulomb branch is completely lifted except for a finite number of discrete vacua. These are found by extremizing the twisted chiral superpotential \mathcal{W} , *i.e.* they are solutions of the twisted chiral ring equations [23, 24]

$$\exp \left(\frac{\partial \mathcal{W}}{\partial \sigma_s^{(I)}} \right) = 1 . \quad (2.17)$$

In order to make contact with the partition of the v.e.v.'s in (2.2), we solve (2.17) about the following classical vacuum:

$$\sigma_{\text{cl}}^{(I)} = \mathcal{A}_1 \oplus \mathcal{A}_2 \oplus \cdots \oplus \mathcal{A}_I . \quad (2.18)$$

Once the solutions to the twisted chiral ring equations are obtained (order by order in the strong coupling scales of the 2d/4d theories), we evaluate the effective twisted chiral superpotential \mathcal{W} on this particular solution, and verify that the non-perturbative contributions exactly coincide with the $\mathcal{W}_{\text{inst}}$ calculated using localization. In essence, this match provides a one-to-one map between 1/2-BPS defects in the 4d gauge theory and massive vacua in the coupled 2d/4d gauge theory.

2.3 A contour from the twisted chiral ring

We now consider in detail the case $M = 4$ corresponding to the quiver in Fig. 2. This is the simplest example that is general enough to contain all relevant features of a generic linear quiver, and thus it serves as a prototypical case.

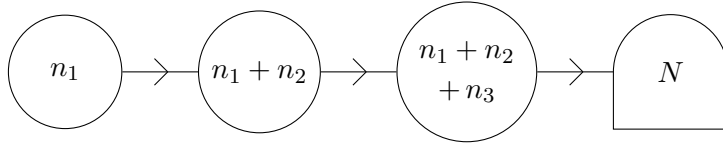


Figure 2. The 4-node linear quiver that corresponds to the partition $[n_1, n_2, n_3, n_4]$.

The twisted chiral ring equations (2.17) can be compactly written in terms of a characteristic gauge polynomial for each $U(r_I)$ node, given by

$$Q_I(z) = \prod_{s=1}^{r_I} (z - \sigma_s^{(I)}) , \quad (2.19)$$

and the characteristic polynomial of the 4d $SU(N)$ node, namely

$$P_N(z) = z^N + \sum_{i=2}^N (-1)^k u_k z^{N-k} , \quad (2.20)$$

where u_k are the gauge invariant coordinates on the moduli space, which can be calculated at weak coupling using localization methods [25–29]. In terms of these polynomials, the twisted chiral equations (2.17) become [10]

$$\begin{aligned} Q_2(\sigma_s^{(1)}) &= \Lambda_1^{n_1+n_2} , \\ Q_3(\sigma_t^{(2)}) &= (-1)^{n_1} \Lambda_2^{n_2+n_3} Q_1(\sigma_t^{(2)}) , \\ P_N(\sigma_u^{(3)}) &= (-1)^{n_1+n_2} \left(\Lambda_3^{n_3+n_4} Q_2(\sigma_u^{(3)}) + \frac{\Lambda_{4d}^{2N}}{\Lambda_3^{n_3+n_4} Q_2(\sigma_u^{(3)})} \right) , \end{aligned} \quad (2.21)$$

for $s \in \mathcal{N}_1$, $t \in \mathcal{N}_1 \cup \mathcal{N}_2$, and $u \in \mathcal{N}_1 \cup \mathcal{N}_2 \cup \mathcal{N}_3$, respectively. We look for solutions of these equations that are of the form

$$\sigma_\star^{(I)} = \sigma_{\text{cl}}^{(I)} + \delta\sigma^{(I)} , \quad (2.22)$$

where the classical part is as in (2.18) for $I = 1, 2, 3$. A detailed derivation of the solution at the one-instanton level is presented in Appendix B. Here we merely write the expressions for the non-vanishing first-order corrections, that are

$$\begin{aligned} \delta\sigma_s^{(1)} &= \frac{\Lambda_1^{n_1+n_2}}{\prod_{r \in \widehat{\mathcal{N}}_1 \cup \mathcal{N}_2} (a_s - a_r)} + \frac{(-1)^{n_2} \Lambda_{4d}^{2N}}{\Lambda_1^{n_1+n_2} \Lambda_2^{n_2+n_3} \Lambda_3^{n_3+n_4} \prod_{r \in \mathcal{N}_4 \cup \widehat{\mathcal{N}}_1} (a_s - a_r)} , \\ \delta\sigma_s^{(2)} = \delta\sigma_s^{(3)} &= \frac{(-1)^{n_2} \Lambda_{4d}^{2N}}{\Lambda_1^{n_1+n_2} \Lambda_2^{n_2+n_3} \Lambda_3^{n_3+n_4} \prod_{r \in \mathcal{N}_4 \cup \widehat{\mathcal{N}}_1} (a_s - a_r)} \end{aligned} \quad (2.23)$$

for $s \in \mathcal{N}_1$,

$$\delta\sigma_t^{(2)} = \frac{(-1)^{n_1} \Lambda_2^{n_2+n_3}}{\prod_{r \in \widehat{\mathcal{N}}_2 \cup \mathcal{N}_3} (a_t - a_r)} \quad (2.24)$$

for $t \in \mathcal{N}_2$, and

$$\delta\sigma_u^{(3)} = \frac{(-1)^{n_1+n_2} \Lambda_3^{n_3+n_4}}{\prod_{r \in \widehat{\mathcal{N}}_3 \cup \mathcal{N}_4} (a_u - a_r)} \quad (2.25)$$

for $u \in \mathcal{N}_3$. In these formulas, the symbol $\widehat{\mathcal{N}}_I$ means that one has to omit from the set \mathcal{N}_I the indices that would yield a vanishing denominator. Even if it is clear by construction, we nevertheless stress that the quantum fluctuations $\delta\sigma^{(I)}$ are non-trivial in the same blocks where the classical values $\sigma_{\text{cl}}^{(I)}$ are non-trivial.

In [10] it was shown that

$$\text{Tr } \sigma_\star^{(I)} = \frac{1}{b_I} \Lambda_I \frac{\partial \mathcal{W}}{\partial \Lambda_I} \Big|_{\sigma_\star} . \quad (2.26)$$

Integrating in this relation, one can obtain the twisted superpotential in the chosen vacuum, which in the one-instanton approximation is

$$\begin{aligned} \mathcal{W}|_{\sigma_*} = & \sum_{s \in \mathcal{N}_1} \frac{\Lambda_1^{n_1+n_2}}{\prod_{r \in \widehat{\mathcal{N}}_1 \cup \mathcal{N}_2} (a_s - a_r)} + \sum_{t \in \mathcal{N}_2} \frac{(-1)^{n_1} \Lambda_2^{n_2+n_3}}{\prod_{r \in \widehat{\mathcal{N}}_2 \cup \mathcal{N}_3} (a_t - a_r)} + \sum_{u \in \mathcal{N}_3} \frac{(-1)^{n_1+n_2} \Lambda_3^{n_3+n_4}}{\prod_{r \in \widehat{\mathcal{N}}_3 \cup \mathcal{N}_4} (a_u - a_r)} \\ & + \sum_{s \in \mathcal{N}_1} \frac{(-1)^{n_2+1} \Lambda_{4d}^{2N}}{\Lambda_1^{n_1+n_2} \Lambda_2^{n_2+n_3} \Lambda_3^{n_3+n_4} \prod_{r \in \mathcal{N}_4 \cup \widehat{\mathcal{N}}_1} (a_s - a_r)} . \end{aligned} \quad (2.27)$$

We now compare this expression with the result of the localization analysis at the one ramified instanton level. From (2.7) and (2.8), specified to the partition $[n_1, \dots, n_4]$, we find

$$Z_{1\text{-inst}} = - \sum_{I=1}^4 q_I \int \frac{d\chi_I}{2\pi i} \frac{1}{\epsilon_1} \prod_{s \in \mathcal{N}_I} \frac{1}{(a_s - \chi_I + \frac{1}{2}(\epsilon_1 + \hat{\epsilon}_2))} \prod_{t \in \mathcal{N}_{I+1}} \frac{1}{(\chi_I - a_t + \frac{1}{2}(\epsilon_1 + \hat{\epsilon}_2))} . \quad (2.28)$$

In view of the prescription (2.9), it is clear that the number of poles that contribute to a given χ_I -integral depends upon whether we close the contour in the upper or lower half-planes. Closing the contour in the upper half-plane leads to n_I poles that contribute, while closing the contour in the lower half-plane leads to n_{I+1} poles that contribute. Furthermore, the mass dimensions of each q_I is fixed to be $n_I + n_{I+1}$, since the partition function itself is dimensionless. These two facts immediately help us in relating the localization results with the chiral ring analysis². Indeed, the dimensional argument allows us to express the ramified instanton counting parameters in terms of the 2d effective scales as follows [10]³:

$$\begin{aligned} q_1 &= (-1)^{n_1} \Lambda_1^{n_1+n_2} , \quad q_2 = (-1)^{n_1+n_2} \Lambda_2^{n_2+n_3} , \\ q_3 &= (-1)^{n_1+n_2+n_3} \Lambda_3^{n_3+n_4} , \quad q_4 = \frac{(-1)^{n_2+n_4} \Lambda^{2N}}{\Lambda_1^{n_1+n_2} \Lambda_2^{n_2+n_3} \Lambda_3^{n_3+n_4}} . \end{aligned} \quad (2.29)$$

Using (2.14), the first three q_I can also be written in terms of the bare complexified FI parameters τ_I of the three 2d nodes as

$$\begin{aligned} q_1 &= e^{2\pi i \tau_1} (-1)^{n_1} \mu^{n_1+n_2} , \\ q_2 &= e^{2\pi i \tau_2} (-1)^{n_1+n_2} \mu^{n_2+n_3} , \\ q_3 &= e^{2\pi i \tau_3} (-1)^{n_1+n_2+n_3} \mu^{n_3+n_4} . \end{aligned} \quad (2.30)$$

Notice that the hierarchy of scales (2.16) implies in this case that the real FI parameters ζ_I are ordered in the following way

$$\zeta_1 \ll \zeta_2 \ll \zeta_3 . \quad (2.31)$$

²In a purely 2d context, a relation between the solution of chiral ring equations for certain quiver theories and contour integrals has been noticed in [30].

³The signs have been chosen to match the two superpotentials exactly.

Once the identification (2.29) is made, we can match the number and the structure of the terms that appear in (2.27) by closing the contours for χ_1 , χ_2 and χ_3 in the upper half-plane, and the contour of χ_4 in the lower half-plane. We denote this choice of contours as $(\chi_1|_+, \chi_2|_+, \chi_3|_+, \chi_4|_-)$. Indeed, computing the corresponding residues and extracting the one-instanton twisted superpotential from (2.10) and (2.28), we find

$$\begin{aligned} \mathcal{W}_{1-\text{inst}} = & \sum_{s \in \mathcal{N}_1} \frac{(-1)^{n_1} q_1}{\prod_{r \in \hat{\mathcal{N}}_1 \cup \mathcal{N}_2} (a_s - a_r)} + \sum_{t \in \mathcal{N}_2} \frac{(-1)^{n_2} q_2}{\prod_{r \in \hat{\mathcal{N}}_2 \cup \mathcal{N}_3} (a_t - a_r)} \\ & + \sum_{u \in \mathcal{N}_3} \frac{(-1)^{n_3} q_3}{\prod_{r \in \hat{\mathcal{N}}_3 \cup \mathcal{N}_4} (a_u - a_r)} + \sum_{s \in \mathcal{N}_1} \frac{(-1)^{n_4+1} q_4}{\prod_{r \in \mathcal{N}_4 \cup \hat{\mathcal{N}}_1} (a_s - a_r)} \end{aligned} \quad (2.32)$$

which, term by term, exactly matches the superpotential (2.27) obtained by solving the twisted chiral ring equations.

3 2d Seiberg duality

The notion of Seiberg duality in 4d gauge theories [18] can be generalized to two dimensions (see for example [19]). Thus, by applying 2d Seiberg duality it is possible to obtain distinct quiver theories in the UV that have the same IR behaviour.

Let us first consider the simplest case, shown in Fig. 3.

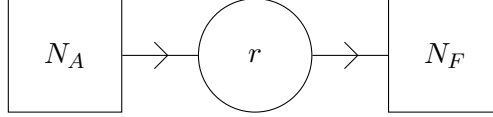


Figure 3. A single 2d gauge node of rank r with N_F fundamental and N_A anti-fundamental flavours attached to it.

This is a 2d $U(r)$ gauge theory with N_F fundamental flavours and N_A anti-fundamental flavours. For definiteness we take $N_F > N_A$, and call this system “theory A”. Its classical twisted superpotential is simply

$$\mathcal{W}_{\text{cl}}^A = 2\pi i \tau \text{Tr } \sigma . \quad (3.1)$$

We now perform a Seiberg duality, and obtain “theory B”, which is described by the quiver in Fig. 4.

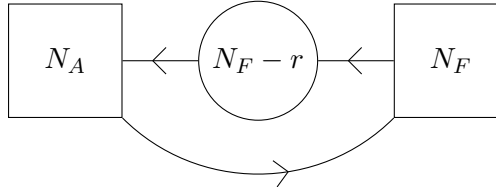


Figure 4. The theory obtained after a 2d Seiberg duality on the gauge node in Fig. 3.

Under the duality, the rank of the gauge group changes as

$$r \longrightarrow r' = \max(N_F, N_A) - r = N_F - r , \quad (3.2)$$

and the roles of the fundamental and anti-fundamental flavours are exchanged as denoted by the reversal of the arrows. The classical twisted superpotential for “theory B” is ⁴

$$\mathcal{W}_{\text{cl}}^{\text{B}} = -2\pi i \tau \text{Tr } \sigma' + 2\pi i \tau \sum_{f=1}^{N_F} m_f \quad (3.3)$$

where σ' denotes the twisted chiral superfield in the vector multiplet of the dualized node and m_f are the twisted masses that completely break the flavour symmetry to its Cartan subgroup.

We now apply this basic duality rule to the quiver theories that describe surface operators. Since for a given 2d node the flavour symmetry is realized by the adjacent nodes, we can encounter two kinds of configurations. The first one is when we dualize a gauge node with both fundamental and anti-fundamental fields in an oriented sequence, as shown in Fig. 5.

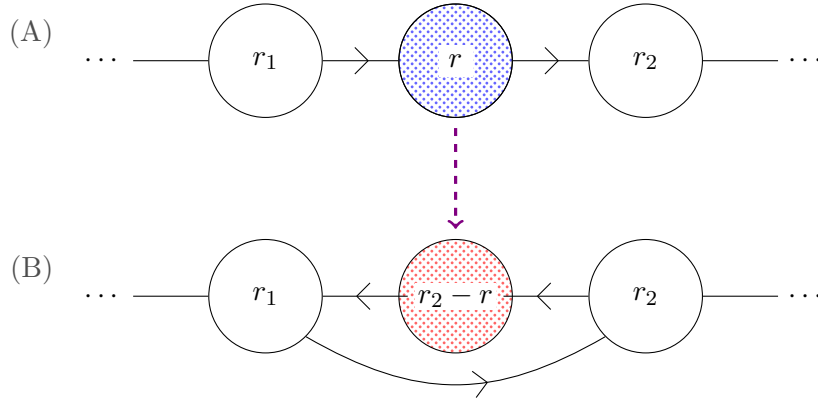


Figure 5. 2d Seiberg duality on a node with both fundamental and anti-fundamental matter with $r_2 > r_1$. The rank of the dualized node is $\max(r_1, r_2) = r_2$. The blue and red colours indicate the node before and after the duality.

Before the duality, the classical superpotential for the three relevant nodes is

$$\mathcal{W}_{\text{cl}}^{\text{A}} = \dots + 2\pi i \tau_1 \text{Tr } \sigma^{(1)} + 2\pi i \tau \text{Tr } \sigma + 2\pi i \tau_2 \text{Tr } \sigma^{(2)} + \dots , \quad (3.4)$$

while, after duality, it becomes

$$\mathcal{W}_{\text{cl}}^{\text{B}} = \dots + 2\pi i \tau_1 \text{Tr } \sigma^{(1)} - 2\pi i \tau \text{Tr } \sigma' + 2\pi i (\tau_2 + \tau) \text{Tr } \sigma^{(2)} + \dots . \quad (3.5)$$

Here we have taken into account the fact that the role of the twisted masses for the dualized node is played by the σ -variables of the r_2 node. This explains why the FI parameter τ_2 is shifted by τ .

⁴In addition, an ordinary superpotential term is generated, but it plays no role in our discussion.

The second possibility is when we dualize a node with only fundamental matter, as shown in Fig. 6. In this case the classical superpotential before the duality is still given by (3.4), but after the duality it becomes

$$\mathcal{W}_{\text{cl}}^{\text{B}} = \dots + 2\pi i (\tau_1 + \tau) \text{Tr } \sigma^{(1)} - 2\pi i \tau \text{Tr } \sigma' + 2\pi i (\tau_2 + \tau) \text{Tr } \sigma^{(2)} + \dots \quad (3.6)$$

because both adjacent nodes provide fundamental matter for the dualized node, and hence both FI parameters τ_1 and τ_2 get shifted by τ .

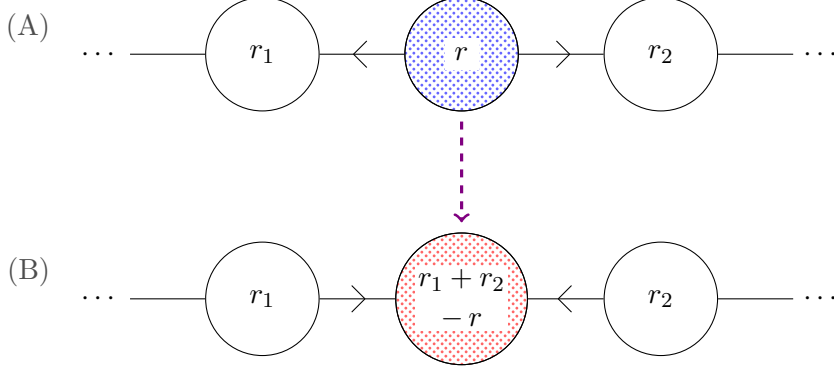


Figure 6. 2d Seiberg duality on a node with only chiral fundamental matter realized by adjacent 2d gauge nodes. In this case there are no mesonic fields introduced in this case.

4 Relating quivers and contours

In this section we discuss different 2d/4d theories related by Seiberg duality to the oriented quiver represented in Fig. 2. To any of these theories we can associate a system of twisted chiral ring equations that are distinct from the ones we have discussed in Section 2.3. However, being related by Seiberg duality, there is a simple one-to-one map among them and their solutions. Then, a natural question arises: how is this duality map reflected on the localization side?

To answer this question, we start by considering again the oriented quiver of Fig. 2, which we now denote by Q_1 . From it we can generate equivalent quivers by dualizing any of the 2d nodes. We first carry out a very specific sequence of dualities that are shown in Fig. 7. This sequence is special because at each step of the duality chain, the node being dualized has only fundamental matter. Therefore, Seiberg duality always acts as in (3.6)⁵.

For each quiver in the chain, we can proceed as we did in Section 2.3 for Q_1 , namely we integrate out the matter multiplets to obtain the effective twisted chiral superpotential, derive from it the twisted chiral ring equations, solve them about a particular massive vacuum order by order in the strong coupling scales, evaluate the superpotential on the corresponding vacuum and finally compare the result with the ramified instanton calculation with a specific integration contour for the χ_I variables. In this program, the choice of

⁵The same sequence of dualities has also been mentioned in [7].

the classical vacuum is the first important piece of information which we have to provide and to which we now turn.

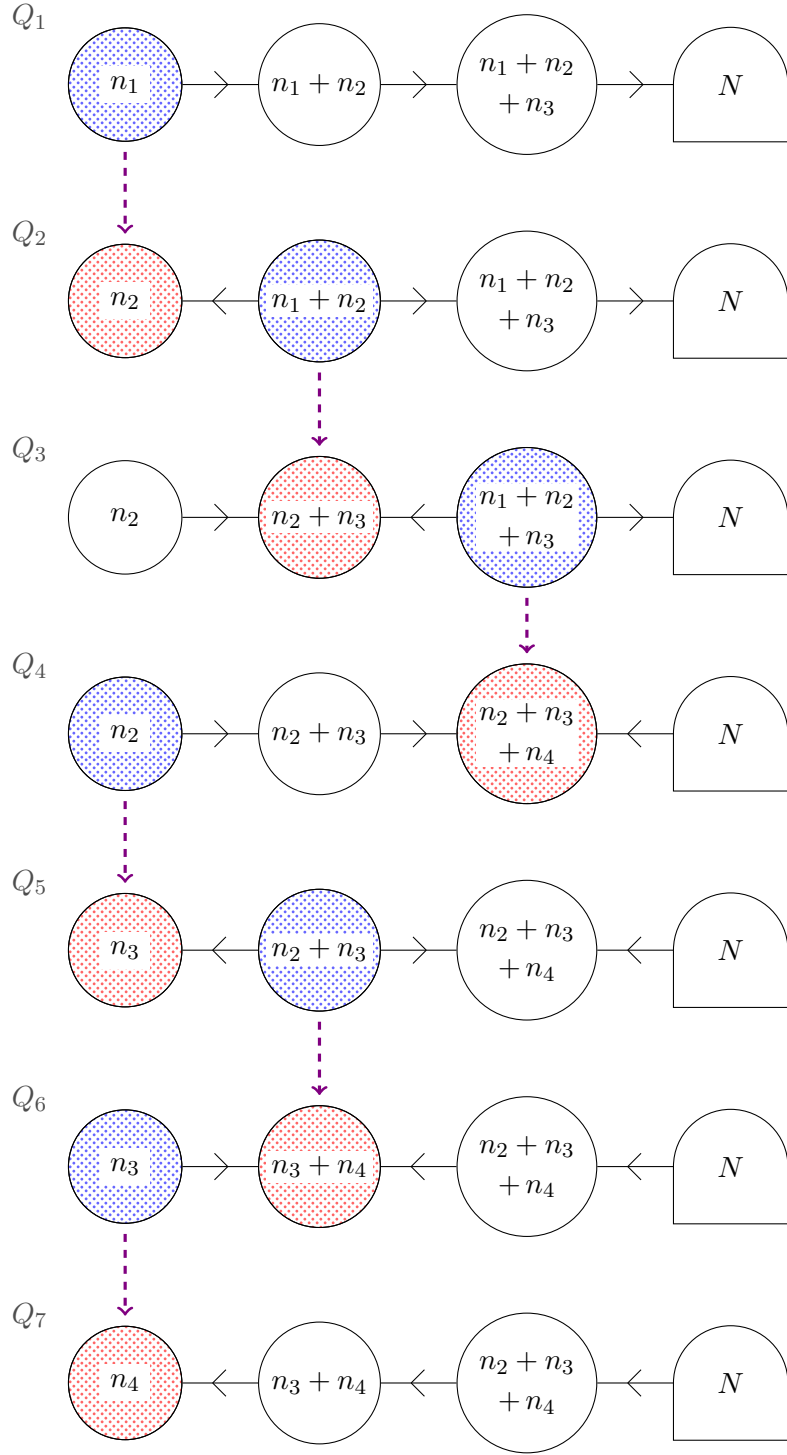


Figure 7. A sequence of Seiberg dualities obtained by dualizing the node that has only fundamental flavours attached to it at each step. The node that is dualized is indicated by the blue arrow.

Classical vacuum

The classical twisted superpotential for the quiver Q_1 is

$$\mathcal{W}_{\text{cl}}^{Q_1} = 2\pi i \tau_1 \text{Tr } \sigma^{(1)} + 2\pi i \tau_2 \text{Tr } \sigma^{(2)} + 2\pi i \tau_3 \text{Tr } \sigma^{(3)} . \quad (4.1)$$

Applying to it the duality rule (3.6), we obtain the classical superpotential for the quiver Q_2 . With a further duality we obtain the classical superpotential for the quiver Q_3 and so on. Explicitly these superpotentials are⁶

$$\begin{aligned} \mathcal{W}_{\text{cl}}^{Q_2} &= -2\pi i \tau_1 \text{Tr } \sigma^{(1)} + 2\pi i (\tau_1 + \tau_2) \text{Tr } \sigma^{(2)} + 2\pi i \tau_3 \text{Tr } \sigma^{(3)} , \\ \mathcal{W}_{\text{cl}}^{Q_3} &= 2\pi i \tau_2 \text{Tr } \sigma^{(1)} - 2\pi i (\tau_1 + \tau_2) \text{Tr } \sigma^{(2)} + 2\pi i (\tau_1 + \tau_2 + \tau_3) \text{Tr } \sigma^{(3)} , \\ \mathcal{W}_{\text{cl}}^{Q_4} &= 2\pi i \tau_2 \text{Tr } \sigma^{(1)} + 2\pi i \tau_3 \text{Tr } \sigma^{(2)} - 2\pi i (\tau_1 + \tau_2 + \tau_3) \text{Tr } \sigma^{(3)} , \\ \mathcal{W}_{\text{cl}}^{Q_5} &= -2\pi i \tau_2 \text{Tr } \sigma^{(1)} + 2\pi i (\tau_2 + \tau_3) \text{Tr } \sigma^{(2)} - 2\pi i (\tau_1 + \tau_2 + \tau_3) \text{Tr } \sigma^{(3)} , \\ \mathcal{W}_{\text{cl}}^{Q_6} &= 2\pi i \tau_3 \text{Tr } \sigma^{(1)} - 2\pi i (\tau_2 + \tau_3) \text{Tr } \sigma^{(2)} - 2\pi i \tau_1 \text{Tr } \sigma^{(3)} , \\ \mathcal{W}_{\text{cl}}^{Q_7} &= -2\pi i \tau_3 \text{Tr } \sigma^{(1)} - 2\pi i \tau_2 \text{Tr } \sigma^{(2)} - 2\pi i \tau_1 \text{Tr } \sigma^{(3)} . \end{aligned} \quad (4.2)$$

From these expressions we can read the map between the effective FI parameters of any quiver and those of the initial quiver Q_1 . For example, for Q_2 we have

$$\tau_1^{\text{eff}} = -\tau_1 , \quad \tau_2^{\text{eff}} = \tau_1 + \tau_2 , \quad \tau_3^{\text{eff}} = \tau_3 , \quad (4.3)$$

while for the quiver Q_3 we have

$$\tau_1^{\text{eff}} = \tau_2 , \quad \tau_2^{\text{eff}} = -\tau_1 - \tau_2 , \quad \tau_3^{\text{eff}} = \tau_1 + \tau_2 + \tau_3 . \quad (4.4)$$

The next step is to identify the classical vacuum for each quiver. We already know that for Q_1 the vacuum that respects the partition $[n_1, \dots, n_4]$ associated to the surface operator is (see (2.18))

$$\sigma_{\text{cl}}^{(1)} = \mathcal{A}_1 , \quad \sigma_{\text{cl}}^{(2)} = \mathcal{A}_1 \oplus \mathcal{A}_2 , \quad \sigma_{\text{cl}}^{(3)} = \mathcal{A}_1 \oplus \mathcal{A}_2 \oplus \mathcal{A}_3 . \quad (4.5)$$

Since Seiberg duality is an exact infrared equivalence, the classical superpotentials of two dual quivers, evaluated in the respective vacua, should be identical. This requirement immediately fixes the structure of the classical vacuum for all quivers. For instance, for Q_2 one can check that

$$\sigma_{\text{cl}}^{(1)} = \mathcal{A}_2 , \quad \sigma_{\text{cl}}^{(2)} = \mathcal{A}_1 \oplus \mathcal{A}_2 , \quad \sigma_{\text{cl}}^{(3)} = \mathcal{A}_1 \oplus \mathcal{A}_2 \oplus \mathcal{A}_3 , \quad (4.6)$$

leads to the desired match; indeed

$$\begin{aligned} \mathcal{W}_{\text{cl}}^{Q_2} &= -2\pi i \tau_1 \text{Tr } \mathcal{A}_2 + 2\pi i (\tau_1 + \tau_2) (\text{Tr } \mathcal{A}_1 + \text{Tr } \mathcal{A}_2) + 2\pi i \tau_3 (\text{Tr } \mathcal{A}_1 + \text{Tr } \mathcal{A}_2 + \text{Tr } \mathcal{A}_3) \\ &= 2\pi i \tau_1 \text{Tr } \mathcal{A}_1 + 2\pi i \tau_2 (\text{Tr } \mathcal{A}_1 + \text{Tr } \mathcal{A}_2) + 2\pi i \tau_3 (\text{Tr } \mathcal{A}_1 + \text{Tr } \mathcal{A}_2 + \text{Tr } \mathcal{A}_3) \\ &= \mathcal{W}_{\text{cl}}^{Q_1} . \end{aligned} \quad (4.7)$$

⁶For ease of notation we use the same symbol $\sigma^{(I)}$ to denote the chiral superfield before and after the duality.

This calculation can be easily generalized to all other quivers in the duality chain and the results are summarized in Tab. 1.

Quiver	$\sigma_{\text{cl}}^{(1)}$	$\sigma_{\text{cl}}^{(2)}$	$\sigma_{\text{cl}}^{(3)}$
Q_1	\mathcal{A}_1	$\mathcal{A}_1 \oplus \mathcal{A}_2$	$\mathcal{A}_1 \oplus \mathcal{A}_2 \oplus \mathcal{A}_3$
Q_2	\mathcal{A}_2	$\mathcal{A}_1 \oplus \mathcal{A}_2$	$\mathcal{A}_1 \oplus \mathcal{A}_2 \oplus \mathcal{A}_3$
Q_3	\mathcal{A}_2	$\mathcal{A}_2 \oplus \mathcal{A}_3$	$\mathcal{A}_1 \oplus \mathcal{A}_2 \oplus \mathcal{A}_3$
Q_4	\mathcal{A}_2	$\mathcal{A}_2 \oplus \mathcal{A}_3$	$\mathcal{A}_2 \oplus \mathcal{A}_3 \oplus \mathcal{A}_4$
Q_5	\mathcal{A}_3	$\mathcal{A}_2 \oplus \mathcal{A}_3$	$\mathcal{A}_2 \oplus \mathcal{A}_3 \oplus \mathcal{A}_4$
Q_6	\mathcal{A}_3	$\mathcal{A}_3 \oplus \mathcal{A}_4$	$\mathcal{A}_2 \oplus \mathcal{A}_3 \oplus \mathcal{A}_4$
Q_7	\mathcal{A}_4	$\mathcal{A}_3 \oplus \mathcal{A}_4$	$\mathcal{A}_2 \oplus \mathcal{A}_3 \oplus \mathcal{A}_4$

Table 1. For each of the quivers in Fig. 7, we list the classical expectation values of the twisted chiral fields in each of the three 2d nodes. Using them in the classical twisted chiral superpotentials given in (4.2), one finds identical expressions.

The q vs Λ map

The next necessary ingredient is the relation between the ramified instanton parameters q_I and the strong coupling scales of a given quiver. For convenience and to avoid unnecessary notational complications, we always use the same symbol Λ_I to denote the strong coupling scale of the I^{th} node of each quiver, even though they are obviously different for different quivers. Furthermore, we always choose the hierarchy (2.16), namely

$$|\Lambda_1| \gg |\Lambda_2| \gg |\Lambda_3| \gg |\Lambda_{4d}| . \quad (4.8)$$

For the first quiver Q_1 the q vs Λ map was already derived and written in (2.29). If we now consider the second quiver Q_2 , from the running of the effective FI parameters and from (2.14), we find

$$\begin{aligned} \Lambda_1^{-n_1-n_2} &= e^{2\pi i \tau_1^{\text{eff}}} \mu^{-n_1-n_2} , \\ \Lambda_2^{n_1+2n_2+n_3} &= e^{2\pi i \tau_2^{\text{eff}}} \mu^{n_1+2n_2+n_3} , \\ \Lambda_3^{n_3+n_4} &= e^{2\pi i \tau_3^{\text{eff}}} \mu^{n_3+n_4} . \end{aligned} \quad (4.9)$$

Using the relations (4.3) and the definitions (2.30), it is easy to obtain (up to inessential signs) the q vs Λ map for Q_2 , namely

$$q_1 \sim \Lambda_1^{n_1+n_2} , \quad q_2 \sim \frac{\Lambda_2^{n_1+2n_2+n_3}}{\Lambda_1^{n_1+n_2}} , \quad q_3 \sim \Lambda_3^{n_3+n_4} . \quad (4.10)$$

Applying the same procedure to Q_3 and using (4.4), we find

$$q_1 \sim \frac{\Lambda_2^{n_1+2n_2+n_3}}{\Lambda_1^{n_2+n_3}} , \quad q_2 \sim \Lambda_1^{n_2+n_3} , \quad q_3 \sim \frac{\Lambda_3^{N+n_2+n_3}}{\Lambda_2^{n_1+2n_2+n_3}} . \quad (4.11)$$

Repeating this analysis for all quivers of Fig. 7, we obtain the results collected in Tab. 2. We finally recall that the following relation

$$q_4 \sim \frac{\Lambda_{4d}^{2N}}{q_1 q_2 q_3} \quad (4.12)$$

holds for all quivers.

Quiver	q_1	q_2	q_3
Q_1	$\Lambda_1^{n_1+n_2}$	$\Lambda_2^{n_2+n_3}$	$\Lambda_3^{n_3+n_4}$
Q_2	$\Lambda_1^{n_1+n_2}$	$\frac{\Lambda_2^{n_1+2n_2+n_3}}{\Lambda_1^{n_1+n_2}}$	$\Lambda_3^{n_3+n_4}$
Q_3	$\frac{\Lambda_2^{n_1+2n_2+n_3}}{\Lambda_1^{n_2+n_3}}$	$\Lambda_1^{n_2+n_3}$	$\frac{\Lambda_3^{N+n_2+n_3}}{\Lambda_2^{n_1+2n_2+n_3}}$
Q_4	$\frac{\Lambda_3^{N+n_2+n_3}}{\Lambda_1^{n_2+n_3} \Lambda_2^{n_3+n_4}}$	$\Lambda_1^{n_2+n_3}$	$\Lambda_2^{n_3+n_4}$
Q_5	$\frac{\Lambda_3^{N+n_2+n_3}}{\Lambda_2^{n_2+2n_3+n_4}}$	$\Lambda_1^{n_2+n_3}$	$\frac{\Lambda_2^{n_2+2n_3+n_4}}{\Lambda_1^{n_2+n_3}}$
Q_6	$\Lambda_3^{n_1+n_2}$	$\frac{\Lambda_2^{n_2+2n_3+n_4}}{\Lambda_1^{n_3+n_4}}$	$\Lambda_1^{n_3+n_4}$
Q_7	$\Lambda_3^{n_1+n_2}$	$\Lambda_2^{n_2+n_3}$	$\Lambda_1^{n_3+n_4}$

Table 2. For each quiver of Fig. 7, we list the q_I vs Λ_I map (up to sign factors, which can be found in Appendix B). The exponents of each strong coupling scale is determined by the number of effective flavours at that node in the quiver.

We observe that except for the oriented quivers Q_1 and Q_7 , in all other cases the contributions of a single ramified instanton can be proportional to the ratio of the strong coupling scales of two adjacent nodes. It would be interesting to understand this fact from the perspective of vortex solutions in 2d quiver with bi-fundamental matter.

4.1 Contour prescriptions for dual quivers

We now address the question of how the non-perturbative superpotential associated to each quiver can be obtained from the ramified instanton partition function (2.7) using a suitable contour prescription for the χ_I -integrals. In Section 2.3 we answered this question for the oriented quiver Q_1 by comparing each term of the solution of the chiral ring equations with the localization results. Here, instead, we provide a general argument that allows one to infer the appropriate contour prescription for any quiver of the duality chain, without explicitly solving the twisted chiral ring equations and integrating them in. We perform a detailed analysis at the one-instanton level, but our conclusions are valid also at higher instantons.

Let us first consider only the three 2d nodes and neglect for the moment the contribution of the 4d node by setting $\Lambda_{4d} \rightarrow 0$ and hence, according to (4.12), $q_4 \rightarrow 0$. Using the

partition function (2.28), the one-instanton superpotential in this case can be written as

$$\mathcal{W}_{1\text{-inst}} = \sum_{I=1}^3 q_I w_I \quad (4.13)$$

where

$$w_I = - \lim_{\epsilon_1, \hat{\epsilon}_2 \rightarrow 0} \int \frac{d\chi_I}{2\pi i} \prod_{s \in \mathcal{N}_I} \frac{1}{(a_s - \chi_I + \frac{1}{2}(\epsilon_1 + \hat{\epsilon}_2))} \prod_{t \in \mathcal{N}_{I+1}} \frac{1}{(\chi_I - a_t + \frac{1}{2}(\epsilon_1 + \hat{\epsilon}_2))} . \quad (4.14)$$

From this we immediately see that w_I can have either n_I or n_{I+1} terms depending on whether the χ_I -contour is closed in the upper or lower half plane, respectively. On the other hand, exploiting the relation [10]

$$\text{Tr } \sigma_\star^{(I)} = \text{Tr } (\sigma_{\text{cl}}^{(I)} + \delta\sigma^{(I)}) = \frac{1}{b_I} \Lambda_I \frac{\partial \mathcal{W}}{\partial \Lambda_I} \Big|_{\sigma_\star} , \quad (4.15)$$

and the maps in Tab. 2, we can understand which type of ramified instantons contributes to each term proportional to $\text{Tr } \sigma^{(I)}$. For example, for Q_1 using the map (2.29), we find

$$\text{Tr } \delta\sigma^{(1)} = q_1 w_1 , \quad \text{Tr } \delta\sigma^{(2)} = q_2 w_2 , \quad \text{Tr } \delta\sigma^{(3)} = q_3 w_3 . \quad (4.16)$$

These relations establish a natural correspondence between the nodes of the quiver and the χ_I fields for $I = 1, 2, 3$: indeed, the first node is associated to χ_1 , the second node to χ_2 and the third node to χ_3 . Furthermore, exploiting the fact that $\delta\sigma^{(I)}$ must have the same structure of the classical part $\sigma_{\text{cl}}^{(I)}$ and hence that their entries can only arise in any of the blocks that make up the rank of the corresponding 2d gauge node, we conclude that we have to close the integration contour in the upper-half plane for all χ_I , so that $\text{Tr } \delta\sigma^{(1)}$ has n_1 contributions, $\text{Tr } \delta\sigma^{(2)}$ has n_2 contributions and $\text{Tr } \delta\sigma^{(3)}$ has n_3 contributions. We indicate this choice of integration contour with the notation $(\chi_1|_+, \chi_2|_+, \chi_3|_+)$. In this way we have retrieved the same contour prescription of Section 2.3, without explicitly solving the twisted chiral ring equations.

The same strategy can be used for the other quivers of the duality chain. Let us consider for example Q_2 . From (4.15) and the map (4.10), we find

$$\text{Tr } \delta\sigma^{(1)} = q_1 w_1 - q_2 w_2 , \quad \text{Tr } \delta\sigma^{(2)} = q_2 w_2 , \quad \text{Tr } \delta\sigma^{(3)} = q_3 w_3 . \quad (4.17)$$

In this case, the correspondence between the second node and χ_2 and between the third node and χ_3 is again obvious, but since now there are two w_I contributing to the first trace, we need to use the hierarchy of scales (4.8) to disentangle the linear combination. In particular we see that the contribution proportional to q_2 is sub-dominant and thus at leading order it can be neglected. This allows us to conclude that the first node must be unambiguously associated to χ_1 . However, the number of terms contributing to $\text{Tr } \delta\sigma^{(1)}$ must be n_2 , since for Q_2 we have $\sigma_{\text{cl}}^{(1)} = \mathcal{A}_2$ (see (4.6)). Thus, the χ_1 -integral should be closed in the lower half-plane to provide this number of terms, while the integrations over χ_2 and χ_3 must be carried out in the upper half-plane as before. In conclusion, to Q_2 we

assign the contour prescription $(\chi_1|-, \chi_2|+, \chi_3|+)$. It can be checked that with this choice the localization results perfectly agree, term by term, with the solution of the appropriate chiral ring equations (see Appendix B for details).

Comparing the classical superpotentials $\mathcal{W}_{\text{cl}}^{Q_1}$ and $\mathcal{W}_{\text{cl}}^{Q_2}$ given in (4.1) and (4.2), we notice that an indication for the flipping of the χ_1 integration contour between Q_1 and Q_2 can be traced to the change in sign of the term containing $\text{Tr } \sigma^{(1)}$, or equivalently to the change in sign of the β -function coefficient b_1 of the first node under the duality map from Q_1 to Q_2 . We propose that this is in fact the rule, and that it is the sign of the β -function coefficient for a given node that determines whether the contour of integration for the corresponding χ variable has to be closed in the upper or in the lower half-plane.

As a simple and non-trivial check of this proposal we consider the quiver Q_3 . Here, using the q vs Λ map of Tab. 2 into (4.15), we find

$$\text{Tr } \delta\sigma^{(1)} = q_2 w_2 - q_1 w_1, \quad \text{Tr } \delta\sigma^{(2)} = q_1 w_1, \quad \text{Tr } \delta\sigma^{(3)} = q_3 w_3. \quad (4.18)$$

From the second and third relations respectively, we see that χ_1 is associated to the second node and χ_3 to the third node. To decide which χ -variable is associated to the first node, we again exploit the hierarchy of scales (4.8), which for the case at hand implies that q_1 is sub-dominant with respect to q_2 . Thus, the q_1 -term in the first relation of (4.4) can be neglected at leading order, implying that χ_2 must be associated to the first node. Notice that it is the second node of Q_3 that has a negative β -function, *i.e.* $b_2 < 0$, and so it is again χ_1 that has to be integrated in the lower half-plane. We then conclude that to the quiver Q_3 we must assign the contour prescription $(\chi_2|+, \chi_1|-, \chi_3|+)$. In writing this prescription, we have ordered the variables from left to right according to the corresponding nodes of the quiver; thus this contour choice is different from the one assigned to Q_2 , because the integrals are computed in a different order. Clearly, this ordering has no relevance at the one-instanton level, but it becomes relevant at higher instantons. A similar analysis can be done for all other quivers of the sequence in Fig. 7.

Let us now turn to the contour for the last integration variable χ_4 . To specify it, we have to switch on the dynamics on the 4d node of the quiver, since the corresponding parameter q_4 is non-zero only when Λ_{4d} is non-zero (see (4.12)). Thus, q_4 and hence χ_4 cannot be associated to any of the 2d nodes and must be related to the 4d node. By observing the duality chain, we see that the third node, which is the only 2d node connected to the 4d node, is dualized precisely once. Until this point the 4d node provides fundamental matter to the third 2d node, while from this point on it provides anti-fundamental matter. Given that we know that for the initial quiver Q_1 the variable χ_4 has to be integrated in the lower half-plane, we are naturally led to propose that the contour for χ_4 remains in the lower plane $(-)$ until the third node is dualized, *i.e.* for Q_1 , Q_2 and Q_3 , and then it flips to the upper half-plane $(+)$, remaining unchanged for the rest of the duality chain, *i.e.* for Q_4 , Q_5 , Q_6 and Q_7 . We have verified the validity of this proposal by explicitly solving the twisted chiral ring equations for all seven quivers to obtain the corresponding twisted superpotentials, and checking that these agree term by term with what the ramified instanton partition function yields with the proposed integration prescriptions (see

Appendix B for details). Our results on the contour assignments for the various quivers are summarized in Tab. 3.⁷

Quiver	$\text{sgn}(b_1)$	$\text{sgn}(b_2)$	$\text{sgn}(b_3)$	contour prescription
Q_1	+	+	+	$(\chi_1 +, \chi_2 +, \chi_3 +, \chi_4 -)$
Q_2	-	+	+	$(\chi_1 -, \chi_2 +, \chi_3 +, \chi_4 -)$
Q_3	+	-	+	$(\chi_2 +, \chi_1 -, \chi_3 +, \chi_4 -)$
Q_4	+	+	-	$(\chi_2 +, \chi_3 +, \chi_1 -, \chi_4 +)$
Q_5	-	+	-	$(\chi_2 -, \chi_3 +, \chi_1 -, \chi_4 +)$
Q_6	+	-	-	$(\chi_3 +, \chi_2 -, \chi_1 -, \chi_4 +)$
Q_7	-	-	-	$(\chi_3 -, \chi_2 -, \chi_1 -, \chi_4 +)$

Table 3. For each quiver in Fig. 7, we list the signs of the β -function coefficients b_I for the three 2d nodes, which determine whether the integration contour for the corresponding χ -variable has to be closed in the upper (+) or lower (-) half-plane. The last column displays the contour prescription from which we can also read which χ -variable is associated to which node of the quiver. The integrals have to be performed in an ordered way, starting from the left-most χ -variable and proceeding rightwards. The variable χ_4 is always the last one to be integrated.

4.2 The Jeffrey-Kirwan prescription for dual quivers

At one-instanton it is sufficient to specify whether the contours of integration for χ_I are closed in the upper or lower half-planes to completely specify the prescription. However, as we already mentioned, at higher instantons this is no longer sufficient since also the order in which the integrations are performed becomes relevant if one wants to have a one-to-one correspondence between the terms appearing in the superpotential derived from the twisted chiral ring equations and the residues contributing in the localization integrals. We have checked in several explicit examples for all quivers of our duality chain, that at two instantons this one-to-one correspondence occurs only if the χ_I -variables in the ramified instanton partition functions are integrated in the order as specified in Tab. 3. Some details on these two-instanton checks are provided in Appendix C.

An elegant way to completely specify the contour of integration is using the Jeffrey-Kirwan (JK) residue prescription [20] (see also, for example, [7, 31, 32] for recent applications to gauge theories). The essential point of this prescription is that the set of poles chosen by a contour is completely specified by the so-called JK reference vector η . For the oriented quiver Q_1 , we propose that the JK reference vector is

$$\eta_{Q_1} = -\zeta_1 \chi_1 - \zeta_2 \chi_2 - \zeta_3 \chi_3 + \zeta_4 \chi_4 , \quad (4.19)$$

⁷We remark that the results of the last quiver Q_7 coincide with those derived in Ref. [10], once the nodes are numbered in the opposite order

where the first three ζ_I are the real FI parameters of the three 2d nodes (see (2.13)) which are related to the magnitude of the corresponding strong coupling scales Λ_I since

$$\left| \frac{\Lambda_I}{\mu} \right|^{b_I} = e^{-2\pi \zeta_I} . \quad (4.20)$$

Similarly, ζ_4 is a parameter that is related to the magnitude of the 4d strong coupling scale Λ_{4d} . The hierarchy of scales (4.8) implies therefore that

$$\zeta_1 \ll \zeta_2 \ll \zeta_3 \ll \zeta_4 . \quad (4.21)$$

Notice that the signs in (4.19) are precisely correlated with the signs appearing in the contour prescription $(\chi_1|_+, \chi_2|_+, \chi_3|_+, \chi_4|_-)$ appropriate for Q_1 . Indeed, one can easily check that the set of poles chosen by the JK vector (4.19) is identical to the one in which the residues in the ramified instanton partition function are taken in the lexicographic order: χ_1 first, followed by χ_2 and so on, as discussed above and also in [7, 10]. We observe that in these references, the JK vector was actually specified with unit coefficients for all χ_I but χ_4 . However, our proposal (4.19) which includes the real FI parameters as coefficients for the first three entries paves the way for a generalization to all other quivers in the duality chain.

It should be clear by now that the essential ingredients are: the hierarchy of scales and the association between the χ_I -integral and traces of a particular gauge node. Once the identification between the χ_I -integral and the gauge node is made, the sign that appears in front of that particular term in the JK vector is correlated with the sign of the β -function coefficient of the corresponding gauge node. Let us see how this works in some examples. For the second quiver Q_2 , our proposal leads to the following JK vector

$$\eta_{Q_2} = +\zeta_1 \chi_1 - \zeta_2 \chi_2 - \zeta_3 \chi_3 + \zeta_4 \chi_4 \quad (4.22)$$

where the ζ_I parameters are still ordered as in (4.21). Note, however, that the sign of the first term has flipped; this is because the χ_1 -integral is associated to the trace of $\sigma^{(1)}$ and the sign of the β -function of the first node flips in going from Q_1 to Q_2 . Again the signs in (4.22) are correlated to the signs appearing in the contour prescription $(\chi_1|_-, \chi_2|_+, \chi_3|_+, \chi_4|_-)$ appropriate for Q_2 .

For the quiver Q_3 we find that the JK vector is

$$\eta_{Q_3} = -\zeta_2 \chi_2 + \zeta_1 \chi_1 - \zeta_3 \chi_3 + \zeta_4 \chi_4 \quad (4.23)$$

where now the ζ_I parameters are ordered as follows

$$\zeta_2 \ll \zeta_1 \ll \zeta_3 \ll \zeta_4 \quad (4.24)$$

as a consequence of q vs Λ map and the hierarchy of scales in this case. Again we see a precise correlation with the contour prescription $(\chi_2|_+, \chi_1|_-, \chi_3|_+, \chi_4|_-)$ which we discussed above for Q_3 . Because of the different ordering of the ζ_I -parameters, the two JK vectors (4.22) and (4.23), which superficially look identical, are actually different. Indeed,

one can check that they select different sets of poles in the calculation of the χ_I integrals (see Appendix C where some examples are worked out for the case of two-instantons).

This procedure can be systematically applied to all quivers in the duality chain and the corresponding JK reference vectors are listed in Tab. 4.

Quiver	JK vector
Q_1	$-\zeta_1 \chi_1 - \zeta_2 \chi_2 - \zeta_3 \chi_3 + \zeta_4 \chi_4$
Q_2	$+\zeta_1 \chi_1 - \zeta_2 \chi_2 - \zeta_3 \chi_3 + \zeta_4 \chi_4$
Q_3	$-\zeta_2 \chi_2 + \zeta_1 \chi_1 - \zeta_3 \chi_3 + \zeta_4 \chi_4$
Q_4	$-\zeta_2 \chi_2 - \zeta_3 \chi_3 + \zeta_1 \chi_1 - \zeta_4 \chi_4$
Q_5	$+\zeta_2 \chi_2 - \zeta_3 \chi_3 + \zeta_1 \chi_1 - \zeta_4 \chi_4$
Q_6	$-\zeta_3 \chi_3 + \zeta_2 \chi_2 + \zeta_1 \chi_1 - \zeta_4 \chi_4$
Q_7	$+\zeta_3 \chi_3 + \zeta_2 \chi_2 + \zeta_1 \chi_1 - \zeta_4 \chi_4$

Table 4. For each quiver we list the JK reference vector that picks the appropriate contour on the localization side. All JK vectors are written such that the ζ_I are ordered with increasing values from left to right.

4.3 Proposal for generic linear quivers

The above analysis for the 4-node case can be extended to quivers with a higher number of nodes in a straightforward manner. Consider a generic linear quiver with M nodes as shown in Fig. 8. Here \tilde{r}_1 always corresponds to one of the entries of the partition \vec{n} that specifies the surface operator, \tilde{r}_2 is the sum of two adjacent entries, and so and so forth, in such a way that $\tilde{r}_1 < \tilde{r}_2 < \dots < \tilde{r}_M$. We have not specified the direction of the arrows connecting the nodes since they can be determined by the sign of the β -function coefficients b_I . Instead, we have highlighted the hierarchy of scales and indicated the χ -variables associated to each node using the notation α_I to denote a permutation of the first $M-1$ integers. As a consequence of the hierarchy of scales and of the q vs Λ map, we have

$$\zeta_{\alpha_1} \ll \zeta_{\alpha_2} \ll \dots \ll \zeta_{\alpha_{M-1}} \ll \zeta_M . \quad (4.25)$$

Then, the contour prescription associated to such a quiver is specified by the following JK reference vector

$$\eta = - \sum_{I=1}^{M-1} \text{sgn}(b_I) \zeta_{\alpha_I} \chi_{\alpha_I} \pm \zeta_M \chi_M \quad (4.26)$$

where the last sign is positive if the 4d gauge node provides fundamental matter to the last 2d node, or negative if it provides anti-fundamental matter. Everything is therefore reduced to finding the permutation α_I that specifies which χ -variable we have to associate to the I^{th} node of the quiver. Of course, this requires a detailed knowledge of the theory but, as we have seen in many examples, it can always be easily done in a systematic manner.

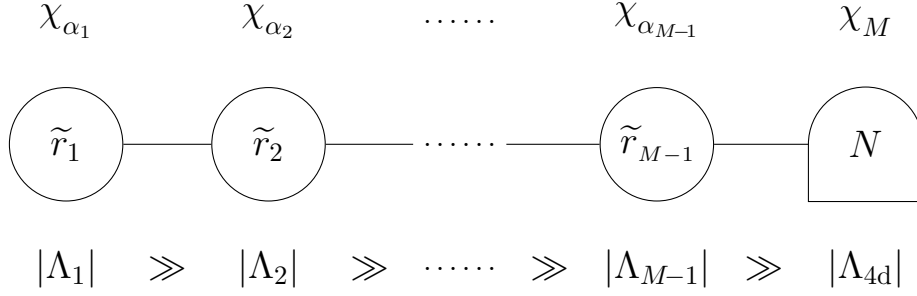


Figure 8. A generic linear quiver with M nodes with ranks r_I representing a generic defect in a 4d $SU(N)$ gauge theory.

5 New quivers and the corresponding contours

The chain of Seiberg dualities shown in Fig. 7 is of a very special kind, since the 2d gauge node being dualized at each step always has only fundamental flavours attached to it. This ensures that the resulting quivers are always linear. We now relax this condition and consider an alternative duality chain with the same initial and final points, but in which we start by dualizing the second node of the quiver Q_1 that has both fundamental and anti-fundamental flavours attached to it. This duality leads to the quiver Q_{2A} which contains a loop, as shown in Fig. 9. Proceeding all the way down as indicated in this figure, we encounter the quivers Q_3 and Q_4 , which were also part of the earlier sequence, but we also find two new quivers, which we call Q_{2B} and Q_{5A} . The latter, like Q_{2A} , contains a loop.

We can repeat the same analysis as before and derive the contour prescription for all quivers in the sequence, including the non-linear ones. The first step is obtaining the classical part of the superpotential. Starting from $\mathcal{W}_{\text{cl}}^{Q_1}$ given in (4.1) and applying the duality rule (3.5) to the second node, we find that the classical part of the superpotential for Q_{2A} is

$$\mathcal{W}_{\text{cl}}^{Q_{2A}} = 2\pi i \tau_1 \text{Tr } \sigma^{(1)} - 2\pi i \tau_2 \text{Tr } \sigma^{(2)} + 2\pi i (\tau_2 + \tau_3) \text{Tr } \sigma^{(3)}. \quad (5.1)$$

If we now dualize the first node of Q_{2A} we obtain the linear quiver Q_{2B} . Here it is natural to relabel the nodes in such a way that the dualized node corresponds to $I = 2$, thus respecting the order shown in Fig. 9. Taking this into account and applying the duality map to (5.1), we then obtain

$$\mathcal{W}_{\text{cl}}^{Q_{2B}} = -2\pi i \tau_2 \text{Tr } \sigma^{(1)} - 2\pi i \tau_1 \text{Tr } \sigma^{(2)} + 2\pi i (\tau_1 + \tau_2 + \tau_3) \text{Tr } \sigma^{(3)}. \quad (5.2)$$

In the next two duality steps we find the quivers Q_3 and Q_4 whose classical superpotentials are given in (4.2). Dualizing the second node of Q_4 , we obtain the non-linear quiver Q_{5A} , whose classical superpotential is

$$\mathcal{W}_{\text{cl}}^{Q_{5A}} = -2\pi i \tau_3 \text{Tr } \sigma^{(1)} + 2\pi i \tau_2 \text{Tr } \sigma^{(2)} - 2\pi i (\tau_1 + \tau_2) \text{Tr } \sigma^{(3)}. \quad (5.3)$$

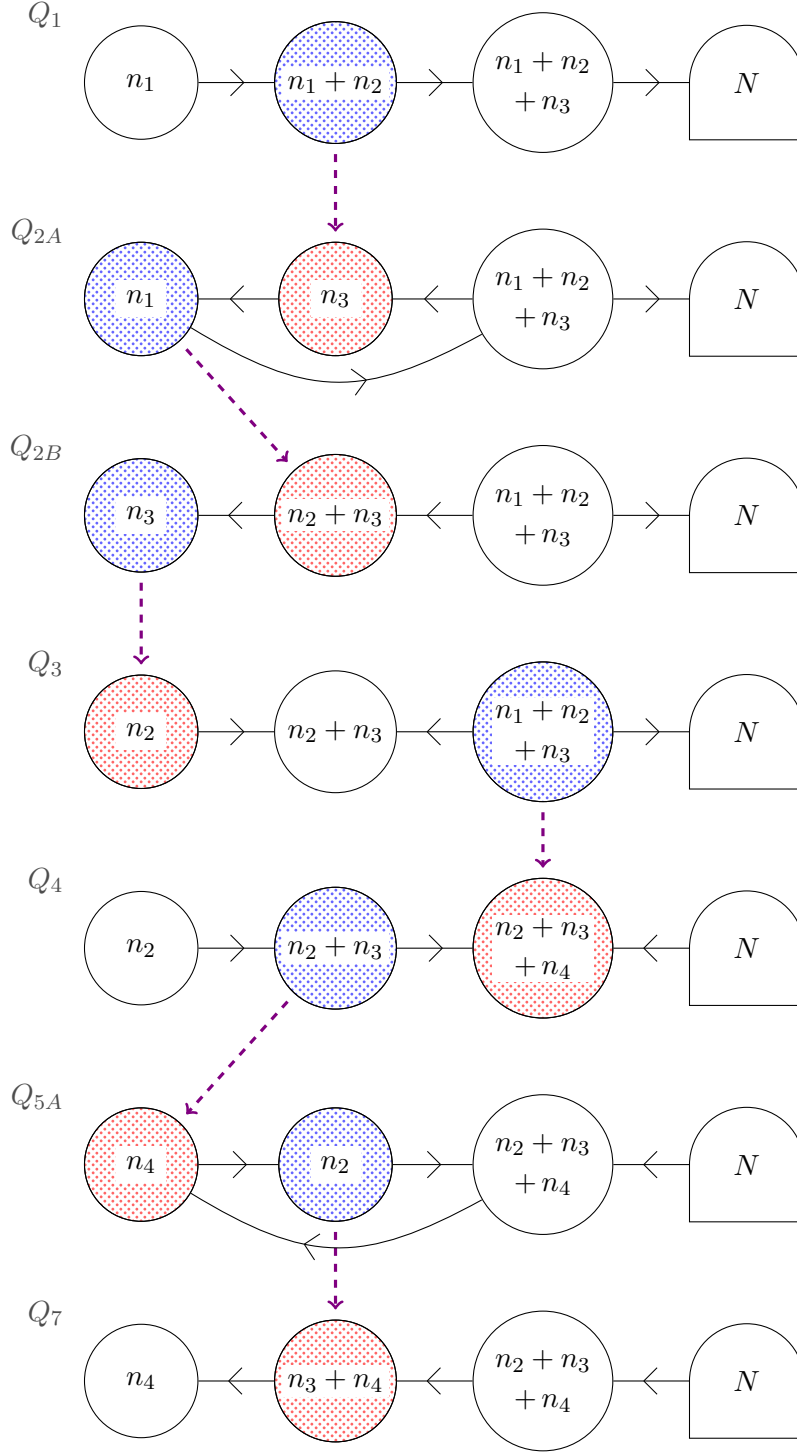


Figure 9. Another chain of dualities to proceed from Q_1 to Q_7 .

Here we have again renamed indices in such a way that the labelling of the σ -variables follows the same order in which the gauge nodes are drawn in Fig. 9.

Next, we determine the classical vacuum for the quivers in this duality chain by equating the classical twisted chiral superpotentials for each dual pairs. In Tab. 5 we report the results for the three new quivers Q_{2A} , Q_{2B} and Q_{5A} of this sequence.

Quiver	$\sigma_{\text{cl}}^{(1)}$	$\sigma_{\text{cl}}^{(2)}$	$\sigma_{\text{cl}}^{(3)}$
Q_{2A}	\mathcal{A}_1	\mathcal{A}_3	$\mathcal{A}_1 \oplus \mathcal{A}_2 \oplus \mathcal{A}_3$
Q_{2B}	\mathcal{A}_3	$\mathcal{A}_2 \oplus \mathcal{A}_3$	$\mathcal{A}_1 \oplus \mathcal{A}_2 \oplus \mathcal{A}_3$
Q_{5A}	\mathcal{A}_4	\mathcal{A}_2	$\mathcal{A}_2 \oplus \mathcal{A}_3 \oplus \mathcal{A}_4$

Table 5. For the quivers Q_{2A} , Q_{2B} and Q_{5A} drawn in Fig. 9, we list the classical expectation values of the twisted chiral fields in each of the 2d nodes, about which one finds the solution to the twisted chiral ring. Using this vacuum along with the effective FI couplings in the classical twisted chiral superpotentials for each of the quivers, one finds identical expressions at leading order. The the vacuum for the other quivers of the duality chain, namely Q_1 , Q_3 , Q_4 and Q_7 can be read from Tab. 1.

Using this information and following the same procedure described in Section 4, we can find the q vs Λ map and the contour prescription that has to be used in the localization formula in order to match term-by-term the superpotential with the one obtained from solving the twisted chiral ring equations. Of course, we do not repeat the derivation of these results since the calculations are a straightforward generalization of what we did for the other duality chain, and we simply collect our findings for the three new quivers Q_{2A} , Q_{2B} and Q_{5A} in Tab. 6. We have checked the validity of our proposal up to two instantons, while some details on the results at the one-instanton level can be found in Appendix B.

Quiver	q_1	q_2	q_3	JK vector
Q_{2A}	$\Lambda_1^{n_1+n_2}$	$\Lambda_2^{n_2+n_3}$	$\frac{\Lambda_3^{n_2+2n_3+n_4}}{\Lambda_2^{n_2+n_3}}$	$-\zeta_1 \chi_1 + \zeta_2 \chi_2 - \zeta_3 \chi_3 + \zeta_4 \chi_4$
Q_{2B}	$\Lambda_2^{n_1+n_2}$	$\Lambda_1^{n_2+n_3}$	$\frac{\Lambda_3^{N+n_2+n_3}}{\Lambda_1^{n_2+n_3} \Lambda_2^{n_1+n_2}}$	$+\zeta_2 \chi_2 + \zeta_1 \chi_1 - \zeta_3 \chi_3 + \zeta_4 \chi_4$
Q_{5A}	$\frac{\Lambda_3^{n_1+2n_2+n_3}}{\Lambda_2^{n_2+n_3}}$	$\Lambda_2^{n_2+n_3}$	$\Lambda_1^{n_3+n_4}$	$+\zeta_3 \chi_3 - \zeta_2 \chi_2 + \zeta_1 \chi_1 - \zeta_4 \chi_4$

Table 6. For the quivers Q_{2A} , Q_{2B} and Q_{5A} drawn in Fig. 9, we list the relations (up to signs) between the ramified instanton counting parameters q_I and the strong coupling scales Λ_I , and also the JK reference vector that selects the contour prescription to be used in computing the ramified instanton partition function using the localization formula.

6 Summary of results

In this paper we have discussed in detail the relation between two distinct realizations of surface operators: as monodromy defects and as coupled 2d/4d quiver gauge theories. The main features of these two points of view and their relations are summarized in Tab. 7.

Monodromy defect	2d/4d quiver models
Partition of N : $[n_1, n_2, \dots, n_M]$	Ranks of 2d gauge nodes
4d Coulomb v.e.v.'s	2d twisted masses
Partition of Coulomb v.e.v.'s	Classical (massive) vacuum
Ramified instanton counting parameters q_I, q_M	2d/4d strong coupling scales Λ_I, Λ_{4d}
$\mathcal{W}_{\text{inst}}(a, q)$	$\mathcal{W}(\sigma, a, \Lambda_I, \Lambda_{4d}) _{\sigma_\star}$
Contour prescription	2d Seiberg duality frame

Table 7. The dictionary between the various features of surface operators in the two descriptions, as monodromy defects and as coupled 2d/4d quivers.

Establishing a precise correspondence between different integration contour prescriptions in the ramified instanton partition function for a monodromy defect and different quiver theories related to each other by a Seiberg duality has been the main focus of our present work. In particular, we have constructed a number of quiver models that have a different ultraviolet realization but share the same infrared physics since the (massive) vacua of their low-energy theories can be mapped onto each other. These massive vacua are obtained by extremizing the effective twisted chiral superpotential of the 2d/4d quiver. The evaluation of the effective superpotential in a particular vacuum is in turn mapped to the twisted superpotential which is extracted from the ramified instanton partition function with a specific contour of integration.

For surface operators in pure $\mathcal{N} = 2$ gauge theories, like the ones we have considered in this paper, residue theorem ensures that one always obtains the same superpotential irrespective of the contour of integration chosen. Nevertheless, by a careful study of the individual residues that contribute to the superpotential, we have been able to map distinct contours on the localization side to distinct Seiberg-dual 2d quivers coupled to the same 4d $SU(N)$ flavour group. The duality frame one chooses affects the details of the other entries in the table above, such as the choice of the classical vacuum and the map between the ramified instanton counting parameters q_I and the strong coupling scales Λ_I . Although we restricted ourselves to systems with four nodes to exhibit our explicit results, it is clear that our analysis can be extended to a generic surface operator in $SU(N)$ gauge theory in a straightforward manner.

There is one caveat to our analysis. All quivers we have studied so far, have only a single 2d node that is connected to the flavour node that is gauged in 4d. It is only for such cases that the coupling of the 2d degrees of freedom to the 4d theory via its resolvent gives results that are consistent with those obtained using localization methods in the monodromy defect approach. It would be very interesting to understand whether quivers with more 2d nodes connected to the 4d node also have an interpretation as surface operators in a 4d gauge theory. Furthermore, there are many worthwhile but yet unexplored directions to pursue, such as the extension of our analysis to (conformal) SQCD models

for which the integrands of ramified instanton partition function may have non-vanishing residues at infinity, or the lift of our techniques to five dimensions to study surface operators from the point of view of 3d/5d coupled systems, with possible Chern-Simons interactions. We leave these extensions and generalizations to future work.

Acknowledgments

We would like to thank Stefano Cremonesi and Amihay Hanany for many useful discussions. S.K.A. would especially like to thank the Physics Department of the University of Torino and the Torino Section of INFN for hospitality during the final stages of this work. M.B., M.F., R.R.J. and A.L. would like to thank the “Galileo Galilei Institute for Theoretical Physics” in Florence for hospitality.

The work of M.B., M.F., R.R.J. and A.L. is partially supported by the MIUR PRIN Contract 2015MP2CX4 “Non-perturbative Aspects Of Gauge Theories And Strings”.

A Localization results at one-instanton level

In this Appendix we collect the localization results at the one-instanton level for the different contours of integrations, corresponding to the different quivers discussed in Sections 4 and 5. The twisted superpotential extracted from the partition function (2.7) is expressed as a sum of residues, and at the one-instanton level it can be easily derived from (2.28).

Integration contour $(\chi_1|_+, \chi_2|_+, \chi_3|_+, \chi_4|_-)$

$$\begin{aligned} \mathcal{W}_{1-\text{inst}} = & \sum_{s \in \mathcal{N}_1} \frac{(-1)^{n_1} q_1}{\prod_{r \in \widehat{\mathcal{N}}_1 \cup \mathcal{N}_2} (a_s - a_r)} + \sum_{t \in \mathcal{N}_2} \frac{(-1)^{n_2} q_2}{\prod_{r \in \widehat{\mathcal{N}}_2 \cup \mathcal{N}_3} (a_t - a_r)} \\ & + \sum_{u \in \mathcal{N}_3} \frac{(-1)^{n_3} q_3}{\prod_{r \in \widehat{\mathcal{N}}_3 \cup \mathcal{N}_4} (a_u - a_r)} + \sum_{s \in \mathcal{N}_1} \frac{(-1)^{n_4+1} q_4}{\prod_{r \in \mathcal{N}_4 \cup \widehat{\mathcal{N}}_1} (a_s - a_r)}. \end{aligned} \quad (\text{A.1})$$

Integration contour $(\chi_1|_-, \chi_2|_+, \chi_3|_+, \chi_4|_-)$:

$$\begin{aligned} \mathcal{W}_{1-\text{inst}} = & \sum_{t \in \mathcal{N}_2} \frac{(-1)^{n_1+1} q_1}{\prod_{r \in \mathcal{N}_1 \cup \widehat{\mathcal{N}}_2} (a_t - a_r)} + \sum_{t \in \mathcal{N}_2} \frac{(-1)^{n_2} q_2}{\prod_{r \in \widehat{\mathcal{N}}_2 \cup \mathcal{N}_3} (a_t - a_r)} \\ & + \sum_{u \in \mathcal{N}_3} \frac{(-1)^{n_3} q_3}{\prod_{r \in \widehat{\mathcal{N}}_3 \cup \mathcal{N}_4} (a_u - a_r)} + \sum_{s \in \mathcal{N}_1} \frac{(-1)^{n_4+1} q_4}{\prod_{r \in \mathcal{N}_4 \cup \widehat{\mathcal{N}}_1} (a_s - a_r)}. \end{aligned} \quad (\text{A.2})$$

Integration contour $(\chi_2|_+, \chi_1|_-, \chi_3|_+, \chi_4|_-)$:

The one-instanton superpotential for this integration contour is the same as in (A.2) since at this order there is no difference between the two cases.

Integration contour $(\chi_2|+, \chi_3|+, \chi_1|-, \chi_4|+)$:

$$\begin{aligned} \mathcal{W}_{1-\text{inst}} = & \sum_{t \in \mathcal{N}_2} \frac{(-1)^{n_1+1} q_1}{\prod_{r \in \mathcal{N}_1 \cup \widehat{\mathcal{N}}_2} (a_t - a_r)} + \sum_{t \in \mathcal{N}_2} \frac{(-1)^{n_2} q_2}{\prod_{r \in \widehat{\mathcal{N}}_2 \cup \mathcal{N}_3} (a_t - a_r)} \\ & + \sum_{u \in \mathcal{N}_3} \frac{(-1)^{n_3} q_3}{\prod_{r \in \widehat{\mathcal{N}}_3 \cup \mathcal{N}_4} (a_u - a_r)} + \sum_{v \in \mathcal{N}_4} \frac{(-1)^{n_4} q_4}{\prod_{r \in \widehat{\mathcal{N}}_4 \cup \mathcal{N}_1} (a_v - a_r)}. \end{aligned} \quad (\text{A.3})$$

Integration contour $(\chi_2|-, \chi_3|+, \chi_1|-, \chi_4|+)$:

$$\begin{aligned} \mathcal{W}_{1-\text{inst}} = & \sum_{t \in \mathcal{N}_2} \frac{(-1)^{n_1+1} q_1}{\prod_{r \in \mathcal{N}_1 \cup \widehat{\mathcal{N}}_2} (a_t - a_r)} + \sum_{u \in \mathcal{N}_3} \frac{(-1)^{n_2+1} q_2}{\prod_{r \in \mathcal{N}_2 \cup \widehat{\mathcal{N}}_3} (a_t - a_r)} \\ & + \sum_{u \in \mathcal{N}_3} \frac{(-1)^{n_3} q_3}{\prod_{r \in \widehat{\mathcal{N}}_3 \cup \mathcal{N}_4} (a_u - a_r)} + \sum_{v \in \mathcal{N}_4} \frac{(-1)^{n_4} q_4}{\prod_{r \in \widehat{\mathcal{N}}_4 \cup \mathcal{N}_1} (a_v - a_r)}. \end{aligned} \quad (\text{A.4})$$

Integration contour $(\chi_3|+, \chi_2|-, \chi_1|-, \chi_4|+)$:

The one-instanton superpotential for this integration contour is the same as in (A.4) since at this order there is no difference between the two cases.

Integration contour $(\chi_3|-, \chi_2|-, \chi_1|-, \chi_4|+)$:

$$\begin{aligned} \mathcal{W}_{1-\text{inst}} = & \sum_{t \in \mathcal{N}_2} \frac{(-1)^{n_1+1} q_1}{\prod_{r \in \mathcal{N}_1 \cup \widehat{\mathcal{N}}_2} (a_t - a_r)} + \sum_{u \in \mathcal{N}_3} \frac{(-1)^{n_2+1} q_2}{\prod_{r \in \mathcal{N}_2 \cup \widehat{\mathcal{N}}_3} (a_u - a_r)} \\ & + \sum_{v \in \mathcal{N}_4} \frac{(-1)^{n_3+1} q_3}{\prod_{r \in \mathcal{N}_3 \cup \widehat{\mathcal{N}}_4} (a_v - a_r)} + \sum_{v \in \mathcal{N}_4} \frac{(-1)^{n_4} q_4}{\prod_{r \in \widehat{\mathcal{N}}_4 \cup \mathcal{N}_1} (a_v - a_r)}. \end{aligned} \quad (\text{A.5})$$

Integration contour $(\chi_1|+, \chi_2|-, \chi_3|+, \chi_4|-)$:

$$\begin{aligned} \mathcal{W}_{1-\text{inst}} = & \sum_{s \in \mathcal{N}_1} \frac{(-1)^{n_1} q_1}{\prod_{r \in \widehat{\mathcal{N}}_1 \cup \mathcal{N}_2} (a_s - a_r)} + \sum_{u \in \mathcal{N}_3} \frac{(-1)^{n_2+1} q_2}{\prod_{r \in \mathcal{N}_2 \cup \widehat{\mathcal{N}}_3} (a_u - a_r)} \\ & + \sum_{u \in \mathcal{N}_3} \frac{(-1)^{n_3} q_3}{\prod_{r \in \widehat{\mathcal{N}}_3 \cup \mathcal{N}_4} (a_u - a_r)} + \sum_{s \in \mathcal{N}_1} \frac{(-1)^{n_4+1} q_4}{\prod_{r \in \mathcal{N}_4 \cup \widehat{\mathcal{N}}_1} (a_s - a_r)}. \end{aligned} \quad (\text{A.6})$$

Integration contour $(\chi_2|-, \chi_1|-, \chi_3|+, \chi_4|-)$:

$$\begin{aligned} \mathcal{W}_{1-\text{inst}} = & \sum_{t \in \mathcal{N}_2} \frac{(-1)^{n_1+1} q_1}{\prod_{r \in \mathcal{N}_1 \cup \widehat{\mathcal{N}}_2} (a_t - a_r)} + \sum_{u \in \mathcal{N}_3} \frac{(-1)^{n_2+1} q_2}{\prod_{r \in \mathcal{N}_2 \cup \widehat{\mathcal{N}}_3} (a_u - a_r)} \\ & + \sum_{u \in \mathcal{N}_3} \frac{(-1)^{n_3} q_3}{\prod_{r \in \widehat{\mathcal{N}}_3 \cup \mathcal{N}_4} (a_u - a_r)} + \sum_{s \in \mathcal{N}_1} \frac{(-1)^{n_4+1} q_4}{\prod_{r \in \mathcal{N}_4 \cup \widehat{\mathcal{N}}_1} (a_s - a_r)}. \end{aligned} \quad (\text{A.7})$$

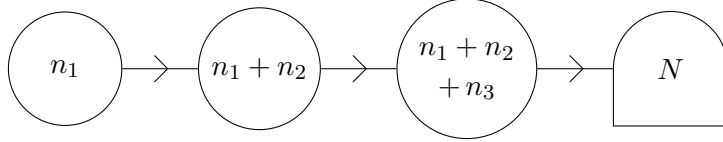
Integration contour $(\chi_3|-, \chi_2|+, \chi_1|-, \chi_4|+)$:

$$\begin{aligned} \mathcal{W}_{1-\text{inst}} = & \sum_{t \in \mathcal{N}_2} \frac{(-1)^{n_1+1} q_1}{\prod_{r \in \mathcal{N}_1 \cup \widehat{\mathcal{N}}_2} (a_t - a_r)} + \sum_{t \in \mathcal{N}_2} \frac{(-1)^{n_2} q_2}{\prod_{r \in \widehat{\mathcal{N}}_2 \cup \mathcal{N}_3} (a_t - a_r)} \\ & + \sum_{v \in \mathcal{N}_4} \frac{(-1)^{n_3+1} q_3}{\prod_{r \in \mathcal{N}_3 \cup \widehat{\mathcal{N}}_4} (a_v - a_r)} + \sum_{u \in \mathcal{N}_4} \frac{(-1)^{n_4} q_4}{\prod_{r \in \widehat{\mathcal{N}}_4 \cup \mathcal{N}_1} (a_u - a_r)} . \end{aligned} \quad (\text{A.8})$$

B Chiral ring equations and superpotentials at the one-instanton level

Quiver Q_1

We begin by considering the first quiver Q_1 of the two duality chains of Fig. 7 and Fig. 9, namely



The corresponding chiral ring equations have already been written in Section 2.3, but we rewrite them here for convenience

$$Q_2(\sigma_s^{(1)}) = \Lambda_1^{n_1+n_2} , \quad (\text{B.1a})$$

$$Q_3(\sigma_t^{(2)}) = (-1)^{n_1} \Lambda_2^{n_2+n_3} Q_1(\sigma_t^{(2)}) , \quad (\text{B.1b})$$

$$P_N(\sigma_u^{(3)}) = (-1)^{n_1+n_2} \left(\Lambda_3^{n_3+n_4} Q_2(\sigma_u^{(3)}) + \frac{\Lambda_{4d}^{2N}}{\Lambda_3^{n_3+n_4} Q_2(\sigma_u^{(3)})} \right) , \quad (\text{B.1c})$$

for $s \in \mathcal{N}_1$, $t \in \mathcal{N}_1 \cup \mathcal{N}_2$, and $u \in \mathcal{N}_1 \cup \mathcal{N}_2 \cup \mathcal{N}_3$, respectively.

We look for solutions of these equations that are of the form $\sigma_\star^{(I)} = \sigma_{\text{cl}}^{(I)} + \delta\sigma^{(I)}$ with the classical vacuum given in the first row of Tab. 1. We work at the lowest order in the quantum fluctuations, proportional to⁸ $\Lambda_1^{n_1+n_2}$, $\Lambda_2^{n_2+n_3}$, $\Lambda_3^{n_3+n_4}$ and $\Lambda_{4d}^{2N}/(\Lambda_1^{n_1+n_2} \Lambda_2^{n_2+n_3} \Lambda_3^{n_3+n_4})$. With this Ansatz, equation (B.1a) gives

$$\delta\sigma_s^{(1)} - \delta\sigma_s^{(2)} = \frac{\Lambda_1^{n_1+n_2}}{\prod_{r \in \widehat{\mathcal{N}}_1 \cup \mathcal{N}_2} (a_s - a_r)} \quad (\text{B.2})$$

for $s \in \mathcal{N}_1$, while equation (B.1b) yields

$$\delta\sigma_t^{(2)} - \delta\sigma_t^{(3)} = \frac{(-1)^{n_1+1} \Lambda_1^{n_1+n_2} \Lambda_2^{n_2+n_3}}{\prod_{u \in \widehat{\mathcal{N}}_1 \cup \mathcal{N}_2 \cup \mathcal{N}_3} (a_t - a_u) \prod_{r \in \mathcal{N}_2} (a_t - a_r)} \quad (\text{B.3})$$

when $t \in \mathcal{N}_1$, and

$$\delta\sigma_t^{(2)} - \delta\sigma_t^{(3)} = \frac{(-1)^{n_1} \Lambda_2^{n_2+n_3}}{\prod_{r \in \widehat{\mathcal{N}}_2 \cup \mathcal{N}_3} (a_t - a_r)} \quad (\text{B.4})$$

⁸According to Table 2 and eq. (4.12) this corresponds to the lowest order in the q_I parameters.

when $t \in \mathcal{N}_2$. The right hand side of (B.3) appears as a higher-order term and hence one could naively think that it may be discarded. However, one should not do that, since it contributes to the lowest-order term in (B.1c).

Let us now consider (B.1c). First of all, we observe that, since we are at the lowest order in the ramified instanton expansion, the quantum polynomial $P_N(z)$ can be replaced with its classical counterpart

$$P_N(z) = \prod_{i=1}^N (z - a_i) . \quad (\text{B.5})$$

Then, we proceed to solve (B.1c) block by block. In the first block when $u \in \mathcal{N}_1$ and $Q_2(\sigma_u^{(3)})$ has a zero, it is the term proportional to Λ_{4d}^{2N} in the right hand side of (B.1c) that contributes to lowest order, and one finds

$$\prod_{r \in \widehat{\mathcal{N}}_1 \cup \mathcal{N}_2 \cup \mathcal{N}_3 \cup \mathcal{N}_4} (a_u - a_r) \delta\sigma_u^{(3)} = \frac{(-1)^{n_1+n_2} \Lambda_{4d}^{2N}}{\Lambda_3^{n_3+n_4} \prod_{r \in \widehat{\mathcal{N}}_1 \cup \mathcal{N}_2} (a_u - a_r) (\delta\sigma_u^{(3)} - \delta\sigma_u^{(2)})} . \quad (\text{B.6})$$

Inserting (B.3), we find

$$\delta\sigma_u^{(3)} = \frac{(-1)^{n_2} \Lambda_{4d}^{2N}}{\Lambda_1^{n_1+n_2} \Lambda_2^{n_2+n_3} \Lambda_3^{n_3+n_4} \prod_{r \in \widehat{\mathcal{N}}_1 \cup \mathcal{N}_4} (a_u - a_r)} . \quad (\text{B.7})$$

In the second block when $u \in \mathcal{N}_2$ and $Q_2(\sigma_u^{(3)})$ has a zero, it is again the term proportional to Λ_{4d}^{2N} in the right hand side of (B.1c) that can contribute to the solution at the lowest order. Indeed, we have

$$\prod_{r \in \mathcal{N}_1 \cup \widehat{\mathcal{N}}_2 \cup \mathcal{N}_3 \cup \mathcal{N}_4} (a_u - a_r) \delta\sigma_u^{(3)} = \frac{(-1)^{n_1+n_2} \Lambda_{4d}^{2N}}{\Lambda_3^{n_3+n_4} \prod_{r \in \mathcal{N}_1 \cup \widehat{\mathcal{N}}_2} (a_u - a_r) (\delta\sigma_u^{(3)} - \delta\sigma_u^{(2)})} . \quad (\text{B.8})$$

Substituting (B.4), we get

$$\delta\sigma_u^{(3)} = \frac{(-1)^{n_2+1} \Lambda_{4d}^{2N}}{\Lambda_2^{n_2+n_3} \Lambda_3^{n_3+n_4} \prod_{r \in \mathcal{N}_1 \cup \widehat{\mathcal{N}}_2 \cup \mathcal{N}_4} (a_u - a_r) \prod_{s \in \mathcal{N}_1} (a_u - a_s)} . \quad (\text{B.9})$$

This term, however, is of higher order and thus can be neglected at the one-instanton level.

Finally, in the third block when $u \in \mathcal{N}_3$ and $Q_2(\sigma_u^{(3)})$ has no zeroes, it is the term proportional to $\Lambda_3^{n_3+n_4}$ in the right hand side of (B.1c) that contributes. Indeed, we find

$$\delta\sigma_u^{(3)} = \frac{(-1)^{n_1+n_2} \Lambda_3^{n_3+n_4}}{\prod_{r \in \widehat{\mathcal{N}}_3 \cup \mathcal{N}_4} (a_u - a_r)} . \quad (\text{B.10})$$

Having obtained the explicit first-order expression for $\delta\sigma^{(3)}$, we can use it in (B.3) and (B.4) to derive the first-order expression for $\delta\sigma^{(2)}$. Explicitly we have

$$\delta\sigma_t^{(2)} = \frac{(-1)^{n_2} \Lambda_{4d}^{2N}}{\Lambda_1^{n_1+n_2} \Lambda_2^{n_2+n_3} \Lambda_3^{n_3+n_4} \prod_{r \in \widehat{\mathcal{N}}_1 \cup \mathcal{N}_4} (a_t - a_r)} \quad (\text{B.11})$$

for $t \in \mathcal{N}_1$, and

$$\delta\sigma_t^{(2)} = \frac{(-1)^{n_1} \Lambda_2^{n_2+n_3}}{\prod_{r \in \widehat{\mathcal{N}}_2 \cup \mathcal{N}_3} (a_t - a_r)} \quad (\text{B.12})$$

for $t \in \mathcal{N}_2$. Further substituting these results in (B.2), we get the first-order expression for $\delta\sigma^{(1)}$, namely

$$\delta\sigma_s^{(1)} = \frac{\Lambda_1^{n_1+n_2}}{\prod_{r \in \widehat{\mathcal{N}}_1 \cup \mathcal{N}_2} (a_s - a_r)} + \frac{(-1)^{n_2} \Lambda_{4d}^{2N}}{\Lambda_1^{n_1+n_2} \Lambda_2^{n_2+n_3} \Lambda_3^{n_3+n_4} \prod_{r \in \widehat{\mathcal{N}}_1 \cup \mathcal{N}_4} (a_s - a_r)} \quad (\text{B.13})$$

for $s \in \mathcal{N}_1$.

Using this explicit solution in (2.26) and integrating in, we obtain that the twisted superpotential in the vacuum is given by

$$\begin{aligned} \mathcal{W}|_{\sigma_*} = & \sum_{s \in \mathcal{N}_1} \frac{\Lambda_1^{n_1+n_2}}{\prod_{r \in \widehat{\mathcal{N}}_1 \cup \mathcal{N}_2} (a_s - a_r)} + \sum_{t \in \mathcal{N}_2} \frac{(-1)^{n_1} \Lambda_2^{n_2+n_3}}{\prod_{r \in \widehat{\mathcal{N}}_2 \cup \mathcal{N}_3} (a_t - a_r)} + \sum_{u \in \mathcal{N}_3} \frac{(-1)^{n_1+n_2} \Lambda_3^{n_3+n_4}}{\prod_{r \in \widehat{\mathcal{N}}_3 \cup \mathcal{N}_4} (a_u - a_r)} \\ & + \sum_{s \in \mathcal{N}_1} \frac{(-1)^{n_2+1} \Lambda_{4d}^{2N}}{\Lambda_1^{n_1+n_2} \Lambda_2^{n_2+n_3} \Lambda_3^{n_3+n_4} \prod_{r \in \mathcal{N}_4 \cup \widehat{\mathcal{N}}_1} (a_s - a_r)} . \end{aligned} \quad (\text{B.14})$$

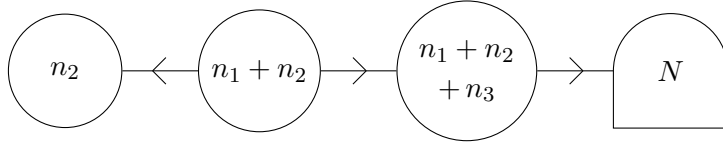
which, term by term, matches the localization result (A.1) if the q vs Λ map is

$$q_1 = (-1)^{n_1} \Lambda_1^{n_1+n_2} , \quad q_2 = (-1)^{n_1+n_2} \Lambda_2^{n_2+n_3} , \quad q_3 = (-1)^{n_1+n_2+n_3} \Lambda_3^{n_3+n_4} \quad (\text{B.15})$$

with $q_1 q_2 q_3 q_4 = (-1)^N \Lambda_{4d}^{2N}$.

Quiver Q_2

Let us now consider the quiver Q_2 :



The corresponding twisted chiral ring equations are

$$Q_2(\sigma_s^{(1)}) = (-1)^{n_1+n_2} \Lambda_1^{n_1+n_2} , \quad (\text{B.16a})$$

$$Q_1(\sigma_t^{(2)}) Q_3(\sigma_t^{(2)}) = \Lambda_2^{n_1+2n_2+n_3} , \quad (\text{B.16b})$$

$$P_N(\sigma_u^{(3)}) = (-1)^{n_1+n_2} \left(\Lambda_3^{n_3+n_4} Q_2(\sigma_u^{(3)}) + \frac{\Lambda_{4d}^{2N}}{\Lambda_3^{n_3+n_4} Q_2(\sigma_u^{(3)})} \right) , \quad (\text{B.16c})$$

for $s \in \mathcal{N}_2$, $t \in \mathcal{N}_1 \cup \mathcal{N}_2$, and $u \in \mathcal{N}_1 \cup \mathcal{N}_2 \cup \mathcal{N}_3$, respectively. The solution of these equations about the classical vacuum indicated in the second row of Tab. 1 is a generalization of what we have discussed in the previous subsection for the quiver Q_1 , and thus we do not repeat

it here. Instead, we write the result of substituting this solution into (2.26) and integrating in, which yields the twisted superpotential in the vacuum, namely

$$\begin{aligned} \mathcal{W}|_{\sigma_*} = & \sum_{t \in \mathcal{N}_2} \frac{(-1)^{n_1+n_2+1} \Lambda_1^{n_1+n_2}}{\prod_{r \in \mathcal{N}_1 \cup \widehat{\mathcal{N}}_2} (a_t - a_r)} + \sum_{t \in \mathcal{N}_2} \frac{(-1)^{n_1+n_2+1} \Lambda_2^{n_1+2n_2+n_3}}{\Lambda_1^{n_1+n_2} \prod_{r \in \widehat{\mathcal{N}}_2 \cup \mathcal{N}_3} (a_t - a_r)} \\ & + \sum_{u \in \mathcal{N}_3} \frac{(-1)^{n_1+n_2} \Lambda_3^{n_3+n_4}}{\prod_{r \in \widehat{\mathcal{N}}_3 \cup \mathcal{N}_4} (a_u - a_r)} + \sum_{s \in \mathcal{N}_1} \frac{(-1)^{n_1+n_2} \Lambda_{4d}^{2N}}{\Lambda_2^{n_1+2n_2+n_3} \Lambda_3^{n_3+n_4} \prod_{r \in \mathcal{N}_4 \cup \widehat{\mathcal{N}}_1} (a_s - a_r)} . \end{aligned} \quad (\text{B.17})$$

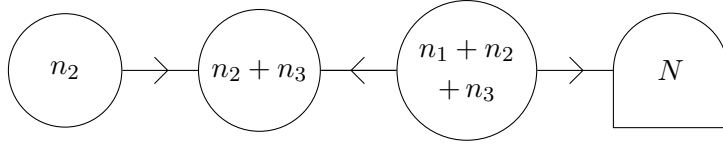
It is easy to see that this exactly matches, term by term, the superpotential (A.2) obtained from localization, if the following q vs Λ map is used

$$q_1 = (-1)^{n_2} \Lambda_1^{n_1+n_2}, \quad q_2 = \frac{(-1)^{n_1+1} \Lambda_2^{n_1+2n_2+n_3}}{\Lambda_1^{n_1+n_2}} \quad q_3 = (-1)^{n_1+n_2+n_3} \Lambda_3^{n_3+n_4} \quad (\text{B.18})$$

with $q_1 q_2 q_3 q_4 = (-1)^N \Lambda_{4d}^{2N}$.

Quiver Q_3

We now consider the quiver Q_3 , namely



The corresponding twisted chiral ring equations are

$$Q_2(\sigma_s^{(1)}) = \Lambda_1^{n_2+n_3} , \quad (\text{B.19a})$$

$$Q_1(\sigma_t^{(2)}) Q_3(\sigma_t^{(2)}) = (-1)^{n_1+n_3} \Lambda_2^{n_1+2n_2+n_3} , \quad (\text{B.19b})$$

$$P_N(\sigma_u^{(3)}) = \frac{\Lambda_3^{N+n_2+n_3}}{Q_2(\sigma_u^{(3)})} + \frac{\Lambda_{4d}^{2N} Q_2(\sigma_u^{(3)})}{\Lambda_3^{N+n_2+n_3}} . \quad (\text{B.19c})$$

for $s \in \mathcal{N}_2$, $t \in \mathcal{N}_2 \cup \mathcal{N}_3$ and $u \in \mathcal{N}_1 \cup \mathcal{N}_2 \cup \mathcal{N}_3$, respectively. Solving them around the vacuum indicated in Tab. 1, plugging the solution into (2.26) and integrating in, we find

$$\begin{aligned} \mathcal{W}|_{\sigma_*} = & \sum_{t \in \mathcal{N}_2} \frac{(-1)^{n_1+n_3} \Lambda_2^{n_1+2n_2+n_3}}{\Lambda_1^{n_2+n_3} \prod_{r \in \mathcal{N}_1 \cup \widehat{\mathcal{N}}_2} (a_t - a_r)} + \sum_{t \in \mathcal{N}_2} \frac{\Lambda_1^{n_2+n_3}}{\prod_{r \in \widehat{\mathcal{N}}_2 \cup \mathcal{N}_3} (a_t - a_r)} \\ & + \sum_{u \in \mathcal{N}_3} \frac{(-1)^{n_1+n_3+1} \Lambda_3^{N+n_2+n_3}}{\Lambda_2^{n_1+2n_2+n_3} \prod_{r \in \widehat{\mathcal{N}}_3 \cup \mathcal{N}_4} (a_u - a_r)} - \sum_{s \in \mathcal{N}_1} \frac{\Lambda_{4d}^{2N}}{\Lambda_3^{N+n_2+n_3} \prod_{r \in \mathcal{N}_4 \cup \widehat{\mathcal{N}}_1} (a_s - a_r)} . \end{aligned} \quad (\text{B.20})$$

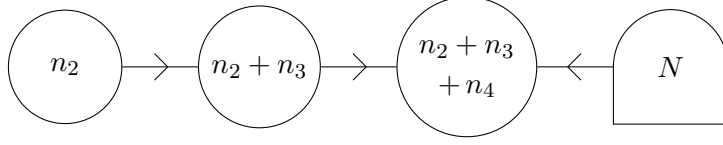
This agrees, term by term, with the localization result (A.2) if the following q vs Λ map is used

$$q_1 = (-1)^{n_3+1} \frac{\Lambda_2^{n_1+2n_2+n_3}}{\Lambda_1^{n_2+n_3}} , \quad q_2 = (-1)^{n_2} \Lambda_1^{n_2+n_3} , \quad q_3 = (-1)^{n_1+1} \frac{\Lambda_3^{N+n_2+n_3}}{\Lambda_2^{n_1+2n_2+n_3}} \quad (\text{B.21})$$

with $q_1 q_2 q_3 q_4 = (-1)^N \Lambda_{4d}^{2N}$.

Quiver Q_4

The quiver Q_4 is



and the corresponding twisted chiral ring equations are

$$Q_2(\sigma_s^{(1)}) = \Lambda_1^{n_2+n_3} , \quad (\text{B.22a})$$

$$Q_3(\sigma_t^{(2)}) = (-1)^{n_2} \Lambda_2^{n_3+n_4} Q_1(\sigma_t^{(2)}) , \quad (\text{B.22b})$$

$$P_N(\sigma_u^{(3)}) = (-1)^{n_1+n_4} \left(\frac{\Lambda_3^{N+n_2+n_3}}{Q_2(\sigma_u^{(3)})} + \frac{\Lambda_{4d}^{2N} Q_2(\sigma_u^{(3)})}{\Lambda_3^{N+n_2+n_3}} \right) \quad (\text{B.22c})$$

for $s \in \mathcal{N}_2$, $t \in \mathcal{N}_2 \cup \mathcal{N}_3$ and $u \in \mathcal{N}_2 \cup \mathcal{N}_3 \cup \mathcal{N}_4$. Proceeding as discussed above, in this case we find

$$\begin{aligned} \mathcal{W}|_{\sigma_*} = & \sum_{t \in \mathcal{N}_2} \frac{(-1)^{n_1+n_2+n_4+1} \Lambda_3^{N+n_2+n_3}}{\Lambda_1^{n_2+n_3} \Lambda_2^{n_3+n_4} \prod_{r \in \mathcal{N}_1 \cup \widehat{\mathcal{N}}_2} (a_t - a_r)} + \sum_{t \in \mathcal{N}_2} \frac{\Lambda_1^{n_2+n_3}}{\prod_{r \in \widehat{\mathcal{N}}_2 \cup \mathcal{N}_3} (a_t - a_r)} \\ & + \sum_{u \in \mathcal{N}_3} \frac{(-1)^{n_2} \Lambda_2^{n_3+n_4}}{\prod_{r \in \widehat{\mathcal{N}}_3 \cup \mathcal{N}_4} (a_u - a_r)} + \sum_{v \in \mathcal{N}_4} \frac{(-1)^{n_1+n_4} \Lambda_{4d}^{2N}}{\Lambda_3^{N+n_2+n_3} \prod_{r \in \widehat{\mathcal{N}}_4 \cup \mathcal{N}_1} (a_v - a_r)} . \end{aligned} \quad (\text{B.23})$$

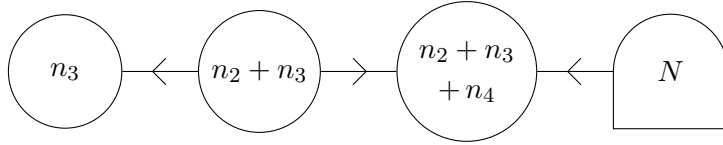
This expression exactly matches, term by term, with the localization result (A.3) provided the following q vs Λ map is used:

$$q_1 = (-1)^{n_2+n_4} \frac{\Lambda_3^{N+n_2+n_3}}{\Lambda_1^{n_2+n_3} \Lambda_2^{n_3+n_4}} , \quad q_2 = (-1)^{n_2} \Lambda_1^{n_2+n_3} , \quad q_3 = (-1)^{n_2+n_3} \Lambda_2^{n_3+n_4} \quad (\text{B.24})$$

with $q_1 q_2 q_3 q_4 = (-1)^N \Lambda_{4d}^{2N}$.

Quiver Q_5

The quiver Q_5 is



and the corresponding twisted chiral ring equations are

$$Q_2(\sigma_s^{(1)}) = (-1)^{n_2+n_3} \Lambda_1^{n_2+n_3} , \quad (\text{B.25a})$$

$$Q_1(\sigma_t^{(2)}) Q_3(\sigma_t^{(2)}) = \Lambda_2^{n_2+2n_3+n_4} , \quad (\text{B.25b})$$

$$P_N(\sigma_u^{(3)}) = (-1)^{n_1+n_4} \left(\frac{\Lambda_3^{N+n_2+n_3}}{Q_2(\sigma_u^{(3)})} + \frac{\Lambda_{4d}^{2N} Q_2(\sigma_u^{(3)})}{\Lambda_3^{N+n_2+n_3}} \right) \quad (\text{B.25c})$$

for $s \in \mathcal{N}_3$, $t \in \mathcal{N}_2 \cup \mathcal{N}_3$ and $u \in \mathcal{N}_2 \cup \mathcal{N}_3 \cup \mathcal{N}_4$ respectively. Solving these equations around the appropriate vacuum (see Tab. 1), using (2.26) and integrating in, we find

$$\begin{aligned} \mathcal{W}|_{\sigma_*} = & \sum_{t \in \mathcal{N}_2} \frac{(-1)^{n_1+n_4} \Lambda_3^{N+n_2+n_3}}{\Lambda_2^{n_2+2n_3+n_4} \prod_{r \in \mathcal{N}_1 \cup \widehat{\mathcal{N}}_2} (a_t - a_r)} + \sum_{u \in \mathcal{N}_3} \frac{(-1)^{n_2+n_3+1} \Lambda_1^{n_2+n_3}}{\prod_{r \in \mathcal{N}_2 \cup \widehat{\mathcal{N}}_3} (a_u - a_r)} \\ & + \sum_{u \in \mathcal{N}_3} \frac{(-1)^{n_2+n_3+1} \Lambda_3^{N+n_2+n_3}}{\Lambda_1^{n_1+n_3} \prod_{r \in \widehat{\mathcal{N}}_3 \cup \mathcal{N}_4} (a_u - a_r)} + \sum_{v \in \mathcal{N}_4} \frac{(-1)^{n_1+n_4} \Lambda_{4d}^{2N}}{\Lambda_3^{N+n_2+n_3} \prod_{r \in \widehat{\mathcal{N}}_4 \cup \mathcal{N}_1} (a_v - a_r)} . \end{aligned} \quad (\text{B.26})$$

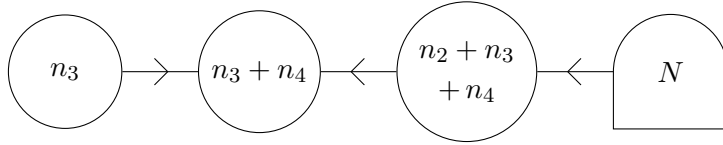
This expression agrees, term by term, with the localization result (A.4) if the following q vs Λ map is used:

$$q_1 = (-1)^{n_4+1} \frac{\Lambda_3^{N+n_2+n_3}}{\Lambda_2^{n_2+2n_3+n_4}} , \quad q_2 = (-1)^{n_3} \Lambda_1^{n_2+n_3} , \quad q_3 = (-1)^{n_2+1} \frac{\Lambda_2^{n_2+2n_3+n_4}}{\Lambda_1^{n_2+n_3}} \quad (\text{B.27})$$

with $q_1 q_2 q_3 q_4 = (-1)^N \Lambda_{4d}^{2N}$.

Quiver Q_6

The quiver Q_6 is



and the corresponding twisted chiral ring equations are

$$Q_2(\sigma_s^{(1)}) = \Lambda_1^{n_3+n_4} , \quad (\text{B.28a})$$

$$Q_1(\sigma_t^{(2)}) Q_3(\sigma_t^{(2)}) = (-1)^{n_2+n_4} \Lambda_2^{n_2+2n_3+n_4} , \quad (\text{B.28b})$$

$$P_N(\sigma_u^{(3)}) = (-1)^N \left(\Lambda_3^{n_1+n_2} Q_2(\sigma_u^{(3)}) + \frac{\Lambda^{2N}}{\Lambda_3^{n_1+n_2} Q_2(\sigma_u^{(3)})} \right) \quad (\text{B.28c})$$

with $s \in \mathcal{N}_3$, $t \in \mathcal{N}_3 \cup \mathcal{N}_4$ and $u \in \mathcal{N}_2 \cup \mathcal{N}_3 \cup \mathcal{N}_4$ respectively. We solve these equations about the classical vacuum given in Tab. 1; after inserting the solution in (2.26) and integrating in, we obtain

$$\begin{aligned} \mathcal{W}|_{\sigma_*} = & \sum_{t \in \mathcal{N}_2} \frac{(-1)^{N+1} \Lambda_3^{n_1+n_2}}{\prod_{r \in \mathcal{N}_1 \cup \widehat{\mathcal{N}}_2} (a_t - a_r)} + \sum_{u \in \mathcal{N}_3} \frac{(-1)^{n_2+n_4} \Lambda_2^{n_2+2n_3+n_4}}{\Lambda_1^{n_3+n_4} \prod_{r \in \mathcal{N}_2 \cup \widehat{\mathcal{N}}_3} (a_u - a_r)} \\ & + \sum_{u \in \mathcal{N}_3} \frac{\Lambda_1^{n_3+n_4}}{\prod_{r \in \widehat{\mathcal{N}}_3 \cup \mathcal{N}_4} (a_u - a_r)} + \sum_{v \in \mathcal{N}_4} \frac{(-1)^{n_1+n_3+1} \Lambda_{4d}^{2N}}{\Lambda_2^{n_2+2n_3+n_4} \Lambda_3^{n_1+n_2} \prod_{r \in \widehat{\mathcal{N}}_4 \cup \mathcal{N}_1} (a_v - a_r)} . \end{aligned} \quad (\text{B.29})$$

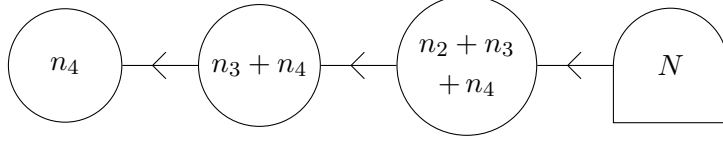
This expression perfectly matches, term by term, the localization result (A.4) if the q vs Λ map is

$$q_1 = (-1)^{n_2+n_3+n_4} \Lambda_3^{n_1+n_2} , \quad q_2 = (-1)^{n_4+1} \frac{\Lambda_2^{n_2+2n_3+n_4}}{\Lambda_1^{n_3+n_4}} , \quad q_3 = (-1)^{n_3} \Lambda_1^{n_3+n_4} \quad (\text{B.30})$$

with $q_1 q_2 q_3 q_4 = (-1)^N \Lambda_{4d}^{2N}$.

Quiver Q_7

The last quiver of the duality chain of in Fig. 7 is



and the associated twisted chiral ring equations are

$$Q_2(\sigma_s^{(1)}) = (-1)^{n_3+n_4} \Lambda_1^{n_3+n_4}, \quad (\text{B.31a})$$

$$Q_3(\sigma_t^{(2)}) = (-1)^{n_2+n_3+n_4} \Lambda_2^{n_2+n_3} Q_1(\sigma_t^{(2)}), \quad (\text{B.31b})$$

$$P_N(\sigma_u^{(3)}) = (-1)^N \left(\Lambda_3^{n_1+n_2} Q_2(\sigma_u^{(3)}) + \frac{\Lambda^{2N}}{\Lambda_3^{n_1+n_2} Q_2(\sigma_u^{(3)})} \right) \quad (\text{B.31c})$$

with $s \in \mathcal{N}_4$, $t \in \mathcal{N}_3 \cup \mathcal{N}_4$ and $u \in \mathcal{N}_2 \cup \mathcal{N}_3 \cup \mathcal{N}_4$. Solving these equation around the vacuum reported in the last row of Tab. 1, and proceeding as in the previous cases, we obtain

$$\begin{aligned} \mathcal{W}|_{\sigma_*} = & \sum_{t \in \mathcal{N}_2} \frac{(-1)^{N+1} \Lambda_3^{n_1+n_2}}{\prod_{r \in \mathcal{N}_1 \cup \widehat{\mathcal{N}}_2} (a_t - a_r)} + \sum_{u \in \mathcal{N}_3} \frac{(-1)^{n_2+n_3+n_4+1} \Lambda_2^{n_2+n_3}}{\prod_{r \in \mathcal{N}_2 \cup \widehat{\mathcal{N}}_3} (a_u - a_r)} \\ & + \sum_{v \in \mathcal{N}_4} \frac{(-1)^{n_3+n_4+1} \Lambda_1^{n_3+n_4}}{\prod_{r \in \mathcal{N}_3 \cup \widehat{\mathcal{N}}_4} (a_v - a_r)} + \sum_{v \in \mathcal{N}_4} \frac{(-1)^{n_1+n_3+n_4} \Lambda_{4d}^{2N}}{\Lambda_1^{n_3+n_4} \Lambda_2^{n_2+n_3} \Lambda_3^{n_1+n_2} \prod_{r \in \widehat{\mathcal{N}}_4 \cup \mathcal{N}_1} (a_v - a_r)}. \end{aligned} \quad (\text{B.32})$$

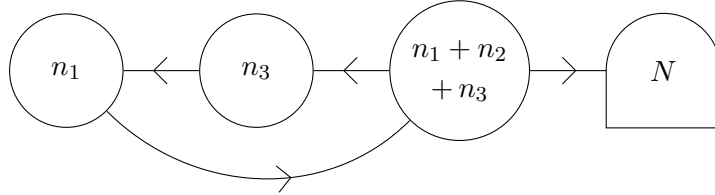
This agrees, term by term, with the localization result (A.5) using the following q vs Λ map

$$q_1 = (-1)^{n_2+n_3+n_4} \Lambda_3^{n_1+n_2}, \quad q_2 = (-1)^{n_3+n_4} \Lambda_2^{n_2+n_3}, \quad q_3 = (-1)^{n_4} \Lambda_1^{n_3+n_4} \quad (\text{B.33})$$

with $q_1 q_2 q_3 q_4 = (-1)^N \Lambda_{4d}^{2N}$.

Quiver Q_{2A}

The non-linear quiver Q_{2A} appearing in the duality chain represented in Fig. 9 is



and its corresponding twisted chiral ring equations are

$$Q_3(\sigma_s^{(1)}) = (-1)^{n_3} \Lambda_1^{n_1+n_2} Q_2(\sigma_s^{(1)}), \quad (\text{B.34a})$$

$$Q_3(\sigma_t^{(2)}) = (-1)^{n_1+n_2+n_3} \Lambda_2^{n_2+n_3} Q_1(\sigma_t^{(2)}), \quad (\text{B.34b})$$

$$P_N(\sigma_u^{(3)}) = (-1)^{n_1} \left(\frac{\Lambda_3^{N+n_3-n_1} Q_1(\sigma_u^{(3)})}{Q_2(\sigma_u^{(3)})} + \frac{\Lambda^{2N} Q_2(\sigma_u^{(3)})}{\Lambda_3^{N+n_3-n_1} Q_1(\sigma_u^{(3)})} \right) \quad (\text{B.34c})$$

for $s \in \mathcal{N}_1$, $t \in \mathcal{N}_3$ and $u \in \mathcal{N}_1 \cup \mathcal{N}_2 \cup \mathcal{N}_3$. Solving them around the vacuum given in the first row of Tab. 5, using (2.26) and integrating in, we obtain

$$\begin{aligned} \mathcal{W}|_{\sigma_*} = & \sum_{s \in \mathcal{N}_1} \frac{(-1)^{n_3} \Lambda_1^{n_1+n_2}}{\prod_{r \in \widehat{\mathcal{N}}_1 \cup \mathcal{N}_2} (a_s - a_r)} + \sum_{u \in \mathcal{N}_3} \frac{(-1)^{n_1+n_2+n_3+1} \Lambda_2^{n_2+n_3}}{\prod_{r \in \mathcal{N}_2 \cup \widehat{\mathcal{N}}_3} (a_u - a_r)} \\ & + \sum_{u \in \mathcal{N}_3} \frac{(-1)^{n_2+n_3+1} \Lambda_3^{n_2+2n_3+n_4}}{\Lambda_2^{n_2+n_3} \prod_{r \in \widehat{\mathcal{N}}_3 \cup \mathcal{N}_4} (a_u - a_r)} + \sum_{s \in \mathcal{N}_1} \frac{(-1)^{n_1+n_3} \Lambda_{4d}^{2N}}{\Lambda_1^{n_1+n_2} \Lambda_3^{n_2+2n_3+n_4} \prod_{r \in \mathcal{N}_4 \cup \widehat{\mathcal{N}}_1} (a_s - a_r)} . \end{aligned} \quad (\text{B.35})$$

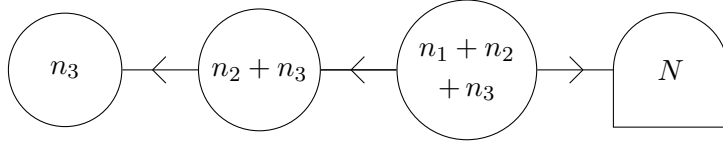
This matches, term by term, the localization result (A.6) using the following q vs Λ map:

$$q_1 = (-1)^{n_1+n_3} \Lambda_1^{n_1+n_2} , \quad q_2 = (-1)^{n_1+n_3} \Lambda_2^{n_2+n_3} , \quad q_3 = (-1)^{n_2+1} \frac{\Lambda_3^{n_2+2n_3+n_4}}{\Lambda_2^{n_2+n_3}} \quad (\text{B.36})$$

with $q_1 q_2 q_3 q_4 = (-1)^N \Lambda_{4d}^{2N}$.

Quiver Q_{2B}

The quiver Q_{2B} is



and its twisted chiral ring equations are

$$Q_2(\sigma_s^{(1)}) = (-1)^{n_2+n_3} \Lambda_1^{n_2+n_3} , \quad (\text{B.37a})$$

$$Q_3(\sigma_t^{(2)}) = (-1)^{n_1+n_2+n_3} \Lambda_2^{n_1+n_2} Q_1(\sigma_t^{(2)}) , \quad (\text{B.37b})$$

$$P_N(\sigma_u^{(3)}) = \frac{\Lambda_3^{N+n_2+n_3}}{Q_2(\sigma_u^{(3)})} + \frac{\Lambda_3^{2N} Q_2(\sigma_u^{(3)})}{\Lambda_3^{N+n_2+n_3}} \quad (\text{B.37c})$$

for $s \in \mathcal{N}_3$, $t \in \mathcal{N}_2 \cup \mathcal{N}_3$ and $u \in \mathcal{N}_1 \cup \mathcal{N}_2 \cup \mathcal{N}_3$, respectively. Solving these equation around the vacuum displayed in the middle row of Tab. 5 and proceeding in the usual way, we get

$$\begin{aligned} \mathcal{W}|_{\sigma_*} = & \sum_{t \in \mathcal{N}_2} \frac{(-1)^{n_1+n_2+n_3+1} \Lambda_2^{n_1+n_2}}{\prod_{r \in \mathcal{N}_1 \cup \widehat{\mathcal{N}}_2} (a_t - a_r)} + \sum_{u \in \mathcal{N}_3} \frac{(-1)^{n_2+n_3+1} \Lambda_1^{n_2+n_3}}{\prod_{r \in \mathcal{N}_2 \cup \widehat{\mathcal{N}}_3} (a_u - a_r)} \\ & + \sum_{u \in \mathcal{N}_3} \frac{(-1)^{n_1} \Lambda_3^{n_2+n_3+N}}{\Lambda_1^{n_2+n_3} \Lambda_2^{n_1+n_2} \prod_{r \in \widehat{\mathcal{N}}_3 \cup \mathcal{N}_4} (a_u - a_r)} - \sum_{s \in \mathcal{N}_1} \frac{\Lambda_{4d}^{2N}}{\Lambda_3^{n_2+n_3+N} \prod_{r \in \mathcal{N}_4 \cup \widehat{\mathcal{N}}_1} (a_s - a_r)} . \end{aligned} \quad (\text{B.38})$$

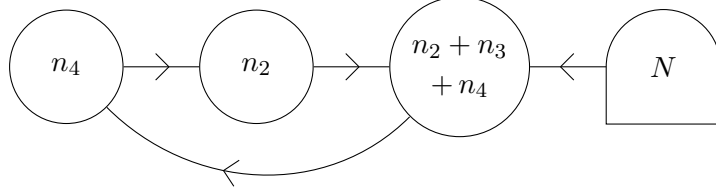
This matches, term by term, the localization result (A.7) using the following q vs Λ map:

$$q_1 = (-1)^{n_2+n_3} \Lambda_2^{n_1+n_2} , \quad q_2 = (-1)^{n_3} \Lambda_1^{n_2+n_3} , \quad q_3 = (-1)^{n_1+n_3} \frac{\Lambda_3^{n_2+n_3+N}}{\Lambda_1^{n_2+n_3} \Lambda_2^{n_1+n_2}} \quad (\text{B.39})$$

with $q_1 q_2 q_3 q_4 = (-1)^N \Lambda_{4d}^{2N}$.

Quiver Q_{5A}

The second non-linear quiver in the duality chain of Fig. 9 is



and the corresponding twisted chiral ring equations are

$$Q_3(\sigma_s^{(1)}) = (-1)^{n_2+n_3+n_4} \Lambda_1^{n_3+n_4} Q_2(\sigma_s^{(1)}) , \quad (\text{B.40a})$$

$$Q_3(\sigma_t^{(2)}) = (-1)^{n_4} \Lambda_2^{n_2+n_3} Q_1(\sigma_t^{(2)}) , \quad (\text{B.40b})$$

$$P_N(\sigma_u^{(3)}) = (-1)^{n_1+n_3+n_4} \left(\frac{\Lambda_3^{n_1+2n_2+n_3} Q_1(\sigma_u^{(3)})}{Q_2(\sigma_u^{(3)})} + \frac{\Lambda^{2N} Q_2(\sigma_u^{(3)})}{\Lambda_3^{n_1+2n_2+n_3} Q_1(\sigma_u^{(3)})} \right) \quad (\text{B.40c})$$

for $s \in \mathcal{N}_4$, $t \in \mathcal{N}_2$ and $u \in \mathcal{N}_2 \cup \mathcal{N}_3 \cup \mathcal{N}_4$, respectively. Solving these equations around the vacuum indicated in the last row of Tab. 5, using (2.26) and integrating in, we find

$$\begin{aligned} \mathcal{W}|_{\sigma_\star} = & \sum_{t \in \mathcal{N}_2} \frac{(-1)^{n_1+n_3} \Lambda_3^{n_1+2n_2+n_3}}{\Lambda_2^{n_2+n_3} \prod_{r \in \mathcal{N}_1 \cup \widehat{\mathcal{N}}_2} (a_t - a_r)} + \sum_{t \in \mathcal{N}_2} \frac{(-1)^{n_4} \Lambda_2^{n_2+n_3}}{\prod_{r \in \widehat{\mathcal{N}}_2 \cup \mathcal{N}_3} (a_t - a_r)} \\ & + \sum_{v \in \mathcal{N}_4} \frac{(-1)^{n_2+n_3+n_4+1} \Lambda_1^{n_3+n_4}}{\prod_{r \in \mathcal{N}_3 \cup \widehat{\mathcal{N}}_4} (a_v - a_r)} + \sum_{v \in \mathcal{N}_4} \frac{(-1)^{n_1+n_2+1} \Lambda_{4d}^{2N}}{\Lambda_1^{n_3+n_4} \Lambda_3^{n_1+2n_2+n_3} \prod_{r \in \widehat{\mathcal{N}}_4 \cup \mathcal{N}_1} (a_v - a_r)} . \end{aligned} \quad (\text{B.41})$$

This superpotential agrees, term by term, with the localization result (A.8) if the q vs Λ map is

$$q_1 = (-1)^{n_3+1} \frac{\Lambda_3^{n_1+2n_2+n_3}}{\Lambda_2^{n_2+n_3}} , \quad q_2 = (-1)^{n_2+n_4} \Lambda_2^{n_2+n_3} , \quad q_3 = (-1)^{n_2+n_4} \Lambda_1^{n_3+n_4} \quad (\text{B.42})$$

with $q_1 q_2 q_3 q_4 = (-1)^N \Lambda_{4d}^{2N}$.

C Some two-instanton results

In this appendix we illustrate how the JK prescription works at two-instantons. In order to keep things as simple as possible, we just focus on the term in the superpotential that is proportional to $q_1 q_2$. After using (2.7) and (2.8), it is not difficult to realize that this term takes the following form

$$\begin{aligned} q_1 q_2 \lim_{\epsilon_1, \hat{\epsilon}_2 \rightarrow 0} \int \frac{d\chi_1}{2\pi i} \frac{d\chi_2}{2\pi i} \frac{1}{(\chi_1 - \chi_2 + \hat{\epsilon}_2)} \prod_{s \in \mathcal{N}_1} \frac{1}{(a_s - \chi_1 + \frac{1}{2}(\epsilon_1 + \hat{\epsilon}_2))} \\ \prod_{t \in \mathcal{N}_2} \frac{1}{(-a_t + \chi_1 + \frac{1}{2}(\epsilon_1 + \hat{\epsilon}_2)) (a_t - \chi_2 + \frac{1}{2}(\epsilon_1 + \hat{\epsilon}_2))} \prod_{u \in \mathcal{N}_3} \frac{1}{(-a_u + \chi_2 + \frac{1}{2}(\epsilon_1 + \hat{\epsilon}_2))} . \end{aligned} \quad (\text{C.1})$$

We now apply the JK prescription to compute the double integral over χ_1 and χ_2 . This amounts to choose two linear factors from the denominator, one containing χ_1 and one containing χ_2 , such that the reference JK vector belongs to the cone defined by the chosen factors. Notice that this way of selecting the residues does not use any information on the Ω -deformation parameters. In Tab. 8 we list the poles that are selected by this JK prescription for the first three quivers Q_1 , Q_2 and Q_3 of the duality chain of Fig. 7.

An important point that we emphasized in the main body of the paper is that the two JK vectors $+\zeta_1 \chi_1 - \zeta_2 \chi_2$ and $-\zeta_2 \chi_2 + \zeta_1 \chi_1$, which superficially look identical, are actually different since $\zeta_1 \ll \zeta_2$ in the first vector, while $\zeta_2 \ll \zeta_1$ in the second vector. Indeed, these two vectors select distinct sets of poles from the integrand as one can explicitly from the entries in the third column of Tab. 8.

Quiver	JK vector	poles
Q_1	$-\zeta_1 \chi_1 - \zeta_2 \chi_2$	$\chi_1 = a_s + \frac{1}{2}(\epsilon_1 + \hat{\epsilon}_2) \quad s \in \mathcal{N}_1$
		$\chi_2 = a_t + \frac{1}{2}(\epsilon_1 + \hat{\epsilon}_2) \quad t \in \mathcal{N}_2$
		$\chi_1 = a_s + \frac{1}{2}(\epsilon_1 + \hat{\epsilon}_2) \quad s \in \mathcal{N}_1$
		$\chi_2 = \chi_1 + \hat{\epsilon}_2$
Q_2	$+\zeta_1 \chi_1 - \zeta_2 \chi_2$	$\chi_1 = a_t - \frac{1}{2}(\epsilon_1 + \hat{\epsilon}_2) \quad t \in \mathcal{N}_2$
		$\chi_2 = a_t + \frac{1}{2}(\epsilon_1 + \hat{\epsilon}_2) \quad t \in \mathcal{N}_2$
		$\chi_1 = a_s + \frac{1}{2}(\epsilon_1 + \hat{\epsilon}_2) \quad s \in \mathcal{N}_1$
		$\chi_2 = \chi_1 + \hat{\epsilon}_2$
		$\chi_1 = \chi_2 - \hat{\epsilon}_2$
Q_3	$-\zeta_2 \chi_2 + \zeta_1 \chi_1$	$\chi_2 = a_t + \frac{1}{2}(\epsilon_1 + \hat{\epsilon}_2) \quad t \in \mathcal{N}_2$
		$\chi_1 = a_t - \frac{1}{2}(\epsilon_1 + \hat{\epsilon}_2) \quad t \in \mathcal{N}_2$
		$\chi_2 = \chi_1 + \hat{\epsilon}_2$
		$\chi_1 = a_t - \frac{1}{2}(\epsilon_1 + \hat{\epsilon}_2) \quad t \in \mathcal{N}_2$
		$\chi_2 = a_u - \frac{1}{2}(\epsilon_1 + \hat{\epsilon}_2) \quad u \in \mathcal{N}_3$
		$\chi_1 = \chi_2 - \hat{\epsilon}_2$

Table 8. We list the poles that contribute to the $q_1 q_2$ term of the superpotential for the first three quivers Q_1 , Q_2 and Q_3 of the duality chain in Fig. 7. In the second column we have shown only the parts of the JK vector that are relevant for this two-instanton contribution. These are written with the ζ_I parameters ordered from left to right according to their magnitudes. Thus, $\zeta_1 \ll \zeta_2$ for Q_1 and Q_2 , and $\zeta_2 \ll \zeta_1$ for Q_3 .

By calculating the residues over the poles selected by the JK vector η_{Q_1} associated to the first quiver Q_1 , we find that the corresponding contribution to the superpotential

proportional to $q_1 q_2$ is

$$\begin{aligned}
w_{q_1 q_2} \Big|_{\eta_{Q_1}} = & - \sum_{s \in \mathcal{N}_1} \frac{(-1)^{n_1+n_2}}{\prod_{r \in \widehat{\mathcal{N}}_1 \cup \mathcal{N}_3} (a_s - a_r) \prod_{t \in \mathcal{N}_2} (a_s - a_t)^2} \\
& - \sum_{\substack{s \in \mathcal{N}_1 \\ t \in \mathcal{N}_2}} \frac{(-1)^{n_1+n_2}}{(a_t - a_s) \prod_{r \in \widehat{\mathcal{N}}_1 \cup \mathcal{N}_2} (a_s - a_r) \prod_{u \in \widehat{\mathcal{N}}_2 \cup \mathcal{N}_3} (a_t - a_u)} .
\end{aligned} \tag{C.2}$$

We have checked that the same result is obtained, term by term, by solving the twisted chiral ring equation of Q_1 at this instanton order and using the appropriate q vs Λ map.

For the second quiver Q_2 , we find

$$\begin{aligned}
w_{q_1 q_2} \Big|_{\eta_{Q_2}} = & - \sum_{s \in \mathcal{N}_1} \frac{(-1)^{n_1+n_2}}{\prod_{r \in \widehat{\mathcal{N}}_1 \cup \mathcal{N}_3} (a_s - a_r) \prod_{t \in \mathcal{N}_2} (a_s - a_t)^2} \\
& + \sum_{\substack{t_1, t_2 \in \mathcal{N}_2 \\ t_1 \neq t_2}} \frac{(-1)^{n_1+n_2}}{(a_{t_1} - a_{t_2}) \prod_{r \in \mathcal{N}_1 \cup \mathcal{N}_3} (a_{t_1} - a_r) \prod_{s \in \widehat{\mathcal{N}}_2} (a_{t_1} - a_s)^2} \\
& + \sum_{s \in \mathcal{N}_1} \sum_{t \in \mathcal{N}_2} \frac{(-1)^{n_1+n_2}}{(a_t - a_s) \prod_{r \in \mathcal{N}_1 \cup \mathcal{N}_3} (a_t - a_r) \prod_{s \in \widehat{\mathcal{N}}_2} (a_t - a_s)^2} \\
& + \sum_{\substack{t_1, t_2 \in \mathcal{N}_2 \\ t_1 \neq t_2}} \frac{(-1)^{n_1+n_2}}{(a_{t_1} - a_{t_2}) \prod_{r \in \widehat{\mathcal{N}}_2 \cup \mathcal{N}_3} (a_{t_1} - a_r) \prod_{s \in \mathcal{N}_1 \cup \widehat{\mathcal{N}}_2} (a_{t_2} - a_s)} .
\end{aligned} \tag{C.3}$$

Similarly, for the third quiver Q_3 we find:

$$\begin{aligned}
w_{q_1 q_2} \Big|_{\eta_{Q_3}} = & + \sum_{u \in \mathcal{N}_3} \frac{(-1)^{n_1+n_2}}{\prod_{r \in \mathcal{N}_1 \cup \widehat{\mathcal{N}}_3} (a_u - a_r) \prod_{t \in \mathcal{N}_2} (a_u - a_t)^2} \\
& - \sum_{\substack{t_1, t_2 \in \mathcal{N}_2 \\ t_1 \neq t_2}} \frac{(-1)^{n_1+n_2}}{(a_{t_1} - a_{t_2}) \prod_{r \in \mathcal{N}_1 \cup \mathcal{N}_3} (a_{t_1} - a_r) \prod_{s \in \widehat{\mathcal{N}}_2} (a_{t_1} - a_s)^2} \\
& - \sum_{t \in \mathcal{N}_2} \sum_{u \in \mathcal{N}_3} \frac{(-1)^{n_1+n_2}}{(a_t - a_u) \prod_{r \in \mathcal{N}_1 \cup \mathcal{N}_3} (a_t - a_r) \prod_{s \in \widehat{\mathcal{N}}_2} (a_t - a_s)^2} \\
& - \sum_{\substack{t_1, t_2 \in \mathcal{N}_2 \\ t_1 \neq t_2}} \frac{(-1)^{n_1+n_2}}{(a_{t_1} - a_{t_2}) \prod_{r \in \mathcal{N}_1 \cup \widehat{\mathcal{N}}_2} (a_{t_1} - a_r) \prod_{s \in \widehat{\mathcal{N}}_2 \cup \mathcal{N}_3} (a_{t_2} - a_s)} .
\end{aligned} \tag{C.4}$$

Once again, we have found perfect agreement, term by term, between these results and those obtained by solving the twisted chiral ring equations for the quivers Q_2 and Q_3 .

References

- [1] S. Gukov, *Surface Operators*, [arXiv:1412.7127](#).
- [2] S. Gukov and E. Witten, *Gauge Theory, Ramification, And The Geometric Langlands Program*, [hep-th/0612073](#).

- [3] S. Gukov and E. Witten, *Rigid Surface Operators*, *Adv. Theor. Math. Phys.* **14** (2010), no. 1 87–178, [[arXiv:0804.1561](#)].
- [4] D. Gaiotto, *Surface Operators in $N = 2$ 4d Gauge Theories*, *JHEP* **11** (2012) 090, [[arXiv:0911.1316](#)].
- [5] D. Gaiotto, S. Gukov, and N. Seiberg, *Surface Defects and Resolvents*, *JHEP* **09** (2013) 070, [[arXiv:1307.2578](#)].
- [6] H. Kanno and Y. Tachikawa, *Instanton counting with a surface operator and the chain-saw quiver*, *JHEP* **06** (2011) 119, [[arXiv:1105.0357](#)].
- [7] A. Gorsky, B. Le Floch, A. Milekhin, and N. Sopenko, *Surface defects and instanton?vortex interaction*, *Nucl. Phys.* **B920** (2017) 122–156, [[arXiv:1702.03330](#)].
- [8] S. K. Ashok, M. Billo, E. Dell’Aquila, M. Frau, R. R. John, and A. Lerda, *Modular and duality properties of surface operators in $N=2^*$ gauge theories*, *JHEP* **07** (2017) 068, [[arXiv:1702.02833](#)].
- [9] S. K. Ashok, M. Billo, E. Dell’Aquila, M. Frau, V. Gupta, R. R. John, and A. Lerda, *Surface operators in 5d gauge theories and duality relations*, *JHEP* **05** (2018) 046, [[arXiv:1712.06946](#)].
- [10] S. K. Ashok, M. Billo, E. Dell’Aquila, M. Frau, V. Gupta, R. R. John, and A. Lerda, *Surface operators, chiral rings and localization in $N=2$ gauge theories*, *JHEP* **11** (2017) 137, [[arXiv:1707.08922](#)].
- [11] L. F. Alday, D. Gaiotto, S. Gukov, Y. Tachikawa, and H. Verlinde, *Loop and surface operators in $N=2$ gauge theory and Liouville modular geometry*, *JHEP* **1001** (2010) 113, [[arXiv:0909.0945](#)].
- [12] L. F. Alday and Y. Tachikawa, *Affine $SL(2)$ conformal blocks from 4d gauge theories*, *Lett. Math. Phys.* **94** (2010) 87–114, [[arXiv:1005.4469](#)].
- [13] E. Witten, *Phases of $N=2$ theories in two-dimensions*, *Nucl. Phys.* **B403** (1993) 159–222, [[hep-th/9301042](#)].
- [14] O. Aharony, A. Hanany, K. A. Intriligator, N. Seiberg, and M. J. Strassler, *Aspects of $N=2$ supersymmetric gauge theories in three-dimensions*, *Nucl. Phys.* **B499** (1997) 67–99, [[hep-th/9703110](#)].
- [15] A. Hanany and K. Hori, *Branes and $N=2$ theories in two-dimensions*, *Nucl. Phys.* **B513** (1998) 119–174, [[hep-th/9707192](#)].
- [16] N. Nekrasov, *BPS/CFT correspondence IV: sigma models and defects in gauge theory*, [[arXiv:1711.11011](#)].
- [17] S. Jeong and N. Nekrasov, *Opers, surface defects, and Yang-Yang functional*, [[arXiv:1806.08270](#)].
- [18] N. Seiberg, *Electric-magnetic duality in supersymmetric non Abelian gauge theories*, *Nucl. Phys.* **B435** (1995) 129–146, [[hep-th/9411149](#)].
- [19] F. Benini, D. S. Park, and P. Zhao, *Cluster Algebras from Dualities of 2d $N = (2, 2)$ Quiver Gauge Theories*, *Commun. Math. Phys.* **340** (2015) 47–104, [[arXiv:1406.2699](#)].
- [20] J. C. Jeffrey and F. C. Kirwan, *Localization for non-abelian actions*, *Topology* **34** (1995) 291–327, [[alg-geom/9307001](#)].

- [21] N. Nekrasov, *Seiberg-Witten prepotential from instanton counting*, *Adv. Theor. Math. Phys.* **7** (2004) 831–864, [[hep-th/0206161](#)].
- [22] N. Nekrasov and A. Okounkov, *Seiberg-Witten theory and random partitions*, *Prog. Math.* **244** (2006) 525–596, [[hep-th/0306238](#)].
- [23] N. A. Nekrasov and S. L. Shatashvili, *Quantum integrability and supersymmetric vacua*, *Prog. Theor. Phys. Suppl.* **177** (2009) 105–119, [[arXiv:0901.4748](#)].
- [24] N. Nekrasov and S. Shatashvili, *Quantization of Integrable Systems and Four Dimensional Gauge Theories*, [arXiv:0908.4052](#).
- [25] U. Bruzzo, F. Fucito, J. F. Morales, and A. Tanzini, *Multi-instanton calculus and equivariant cohomology*, *JHEP* **05** (2003) 054, [[hep-th/0211108](#)].
- [26] A. S. Losev, A. Marshakov, and N. A. Nekrasov, *Small instantons, little strings and free fermions*, [hep-th/0302191](#).
- [27] R. Flume, F. Fucito, J. F. Morales, and R. Poghossian, *Matone’s relation in the presence of gravitational couplings*, *JHEP* **04** (2004) 008, [[hep-th/0403057](#)].
- [28] M. Billo, M. Frau, F. Fucito, L. Giacone, A. Lerda, J. F. Morales, and D. Ricci-Pacifici, *Non-perturbative gauge/gravity correspondence in $N=2$ theories*, *JHEP* **1208** (2012) 166, [[arXiv:1206.3914](#)].
- [29] S. K. Ashok, M. Billo, E. Dell’Aquila, M. Frau, A. Lerda, M. Moskovic, and M. Raman, *Chiral observables and S -duality in $N = 2^* U(N)$ gauge theories*, *JHEP* **11** (2016) 020, [[arXiv:1607.08327](#)].
- [30] D. Orlando and S. Reffert, *Relating Gauge Theories via Gauge/Bethe Correspondence*, *JHEP* **1010** (2010) 071, [[arXiv:1005.4445](#)].
- [31] F. Benini, R. Eager, K. Hori, and Y. Tachikawa, *Elliptic genera of two-dimensional $N=2$ gauge theories with rank-one gauge groups*, *Lett. Math. Phys.* **104** (2014) 465–493, [[arXiv:1305.0533](#)].
- [32] K. Hori, H. Kim, and P. Yi, *Witten Index and Wall Crossing*, *JHEP* **01** (2015) 124, [[arXiv:1407.2567](#)].